https://doi.org/10.5194/bg-2021-232
Preprint. Discussion started: 3 September 2021

Biogeosciences Discussions
Open Access
EGU

Intact polar lipids in the hadal seabed of the Atacama Trench point to lateral sediment transport and *in situ* production as key sources of labile organic matter

Edgart Flores[1,2,3]*, Sebastian I. Cantarero[4], Paula Ruiz-Fernández[1,2,3], Nadia Dildar[4], Matthias Zabel[5], Osvaldo Ulloa[2,3] and Julio Sepúlveda[3,4]*

[1]Programa de Postgrado en Oceanografía, Departamento de Oceanografía, Facultad de Ciencias Naturales y Oceanográficas, Universidad de Concepción, Concepción, Chile
[2]Departamento de Oceanografía, Universidad de Concepción, Casilla 160-C, Concepción, Chile
[3]Millennium Institute of Oceanography, Universidad de Concepción, Concepción, Chile
[4]Department of Geological Sciences and Institute of Arctic and Alpine Research, University of Colorado Boulder, Boulder, CO 80309, USA
[5]MARUM – Center for Marine Environmental Sciences & Department of Geosciences, Univ. of Bremen, D-28334, Bremen, Germany

Correspondence to: Edgart Flores (edgart.flores@imo-chile.cl), Julio Sepúlveda (jsepulveda@colorado.edu)

Abstract. Elevated concentrations of organic matter are found in sediments of hadal trenches relative to those found in the abyssal seabed, but the origin of such biological material remains elusive. Here, we report the composition and distribution of cell membrane intact polar lipids (IPLs) in surface sediments around the deepest points of the Atacama Trench and adjacent bathyal depths to assess and constrain the sources of labile organic matter in the hadal seabed. Multiscale bootstrap resampling of IPLs' structural diversity and abundance indicates distinct lipid signatures in the sediments of the Atacama Trench that are more closely related to those found in bathyal sediments than to those previously reported for the upper ocean water column in the region. While the overall number of unique IPL structures in hadal sediments is limited and they contribute a small fraction of the total IPL pool, they include a high contribution of phospholipids with mono- and di-unsaturated fatty acids that are not associated with photoautotrophic sources. The diversity of labile IPLs in hadal sediments of the Atacama Trench suggests the presence of *in situ* microbial production and biomass that resembles traits of physiological adaptation to high pressure and low temperature, and/or the transport of labile organic matter from shallower sediment. We argue that the export of the most labile lipid component of the organic matter pool from the euphotic zone and the overlying oxygen minimum zone into the hadal sediments is neglectable. Our results contribute to the understanding of the mechanisms that control the delivery of labile organic matter to this extreme deep-sea ecosystem, whereas they provide insights into some potential physiological adaptation of the *in situ* microbial community to high pressure and low temperature through lipid remodeling.

1. Introduction

The deep ocean has been classically considered a vast "biological desert" (Danovaro et al., 2003) due to the attenuation of organic matter fluxes with increasing ocean depth (Wakeham et al., 1984; Martin et al., 1987;

https://doi.org/10.5194/bg-2021-232
Preprint. Discussion started: 3 September 2021

Hedges et al., 2001; Rex et al., 2006). However, hadal trenches (~6,000-11,000 m below sea level) contradict this long-held paradigm (Danovaro et al., 2003; Glud et al., 2013; Leduc et al., 2016; Wenzhöfer et al., 2016; Luo et al., 2017) as they act as depocenters of organic matter (Jahnke and Jahnke, 2000) and hotspots for microbial activity (Glud et al., 2013; Wenzhöfer et al., 2016; Liu et al., 2019). In hadal trench systems, while hydrostatic pressure appears to be the most important physical factor controlling biological activity compared to shallower habitats (Jamieson et al., 2010; Tamburini et al., 2013), the availability of organic matter has been considered the major factor controlling the abundance, biomass, and diversity of life in the deep ocean (Danovaro et al., 2003; Ichino et al., 2015). However, our knowledge on the composition and potential sources of organic matter in marine trenches remains limited. A study by Xu et al. (2018) indicates that the main sources of organic matter to the hadal zone are: (1) the vertical sinking of particulate organic matter; (2) the carrion falls of dead bodies; (3) inputs of terrestrial organic matter; (4) lateral transport of organic matter from continental slopes under the combined effects of trench topography and gravity (Jahnke et al., 1990; Fischer et al., 2009; Inthorn et al., 2006; Ichino et al., 2015), or by earthquakes (Glud et al., 2013; Kioka et al., 2019); and (5) *in situ* chemosynthetic production associated with cold seeps or hydrothermal vents. Previous studies have highlighted the importance of particulate organic matter sinking mainly from the euphotic zone (Stockton and DeLaca, 1982; Angel, 1984; Gooday et al., 2010). In fact, the settling flux of particulate matter measured by sediment traps at 4,000 m of depth in the North Pacific Subtropical Gyre Ocean reveals that a seasonal export pulse can exceed the mean annual flux by ~150% (Poff et al., 2021). However, it is unknown whether such pulses reach the hadal sediments (6,000-11,000 m) with the same intensity and impact. Independent of the main sources of organic matter, which can vary spatially and temporally, the channeling of allochthonous organic matter to the hadal zone should be facilitated by the characteristic V-shape cross-section of trenches (Itou et al., 2000; Itoh et al., 2011; Bao et al., 2018). Additionally, autochthonous sources of organic matter associated with *in situ* bacterial and archaeal biomass production may exist (Smith, 2012; Nunoura et al., 2016; Ta et al., 2019; Hand et al., 2020), but their overall contribution as a secondary input to carbon budgets and energy flow in these systems remains poorly constrained. The spatial differences seen in benthic prokaryotic populations in hadal regions such as the Mariana, Japan, and Izu-Ogasawara trenches have been attributed to the variability of biogeochemical conditions, mainly nitrate and oxygen (Hiraoka et al., 2020), with the latter showing large variability in its consumption (Glud et al., 2021). Furthermore, the abundance of prokaryotes in hadal depths can be influenced by sediment redistribution (Schauberger et al., 2021), which in turn may be influenced by the intensity of propagating internal tides (Turnewitsch et al., 2014). All these factors likely alter the deposition, distribution, and composition of organic matter present in trench sediments.

Recent metagenomic studies have revealed the presence of abundant heterotrophic microorganisms in sediments of the Challenger Deep (Nunoura et al., 2018), which are likely fueled by the endogenous recycling of available organic matter (Nunoura et al., 2015; Tarn et al., 2016). Although less specific than genomic markers, cell membrane intact polar lipids (IPLs) allow more quantitative estimates of microbial biomass in nature (e.g., Lipp et al., 2008; Schubotz et al., 2009; Cantarero et al., 2020). IPLs are composed of a polar head group typically attached to a glycerol backbone from which aliphatic chains are attached via ester and/or ether bonds (Sturt et al., 2004). Their structural diversity is given by the modifications found in the different components of their chemical structure (e.g., polar head groups can be comprised of phosphorous, nitrogen, sulfur, sugars, and amino acids), whereas aliphatic chains (alkyl or isoprenoidal) can vary in their length (number of carbon atoms), and their degree of unsaturation, methylation, hydroxylation, and cyclization (Van Mooy and Fredricks, 2010; Brandsma et al.,

https://doi.org/10.5194/bg-2021-232
Preprint. Discussion started: 3 September 2021

2011; Schubotz et al., 2013). In bacteria and eukarya, alkyl chains are most commonly linked via an ester bond to the sn-glycerol-3-phosphate backbone (Koga and Morii, 2007), although some bacteria are known to produce di- and tetraether lipids (Weijers et al., 2007). Archaea produce membranes rich in di- and tetraether isoprenoidal lipids (Volkman et al., 1989; Pearson and Ingalls, 2013), where isoprenoids are linked via an ether bond to the *sn*-glycerol-1-phosphate backbone (Jain et al., 2014). The variability of membrane chemical structures underlies the adaptability of microbial lifestyles to changing environmental conditions such as nutrients, temperature, oxygen, pH, and pressure (DeLong and Yayanos, 1985; Somero, 1992; Van Mooy et al., 2009; Carini et al., 2015; Sebastián et al., 2016; Siliakus et al., 2017; Boyer et al., 2020). Furthermore, since eukaryotic and bacterial ester-bond IPLs are more labile than ether-bond counterparts (Logemann et al., 2011), they are suitable biomarkers to evaluate sources of labile organic matter in marine environments.

IPLs have been previously used as microbial markers in diverse marine settings, such as along strong redox gradients in the Black Sea (Schubotz et al., 2009b) and the oxygen minimum zones (OMZs) of the eastern tropical Pacific (Schubotz et al., 2018a; Cantarero et al., 2020) and the Arabian Sea (Pitcher, 2011), as well as in surface open ocean waters of the eastern south Pacific (Van Mooy and Fredricks, 2010), the northwestern Atlantic (Popendorf et al., 2011b), and the Mediterranean Sea (Popendorf et al., 2011a), to name a few. Their utility as markers of microbial diversity and processes has also been tested in marine sediments (Liu et al., 2011, 2012; Sturt et al., 2004), such as along the Peru Margin, Equatorial Pacific, Hydrate Ridge, and Juan de Fuca Ridge (Lipp and Hinrichs, 2009a) and in subsurface sediment layers from the Peru Margin (Biddle et al., 2006). However, to the best of our knowledge, no IPL studies have been reported for sediments of hadal trenches.
In this study, we investigate the chemical diversity and abundance of microbial IPLs as markers of labile organic matter sources in the deepest points of the Atacama Trench sediments (AT), and compare them to similar IPL stocks in shallower surface sediments (~500-1,200 m) and in the overlying water column (upper 700 m; Cantarero et al., 2020). More specifically, we evaluate possible organic matter provenance (*in situ* vs. allochthonous production) and some potential chemical adaptations of the *in situ* microbial community to the extreme conditions of the hadal region.

2. Material and Methods

2.1. Study areas and sampling

The AT is located in the eastern tropical South Pacific (ETSP) along the Peru-Chile margin, and it underlies the eutrophic and highly productive Humboldt Current System (Angel, 1982; Ahumada, 1989), which includes the fourth largest (by volume) oxygen minimum zone (OMZ) in the world (Schneider et al., 2006). In this area, while there is minimal river runoff (Houston, 2006), winds can transfer dust from the adjacent continental desert (Angel, 1982). With an extension of ~5,900 km, the AT is the world's largest trench (Sabbatini et al., 2002), whereas it is geographically isolated from other trenches in the Pacific Ocean.

In this study, we investigated the diversity and abundance of IPLs in a total of 9 hadal surface sediments (3 sites between 7,734 and 8,063 m water depth, with 3 depth intervals each) collected during the HADES-SO261 cruise (March to April 2018) onboard the RV *Sonne* (Wenzhöfer, 2019) , and 7 bathyal surface sediments (7 sites; 529-1200 m water depth) collected during the ChiMeBo-SO211 cruise (November 2-29, 2010) onboard the RV *Sonne*

https://doi.org/10.5194/bg-2021-232
Preprint. Discussion started: 3 September 2021

(Matys et al., 2017) (Table 1; Fig. 1). We compare our results against IPL results from the overlying water column (0-700 m) recently reported in Cantarero et al. (2020).

Table 1. Sampling stations from the Hades, ChiMeBo, and LowpHOX-2 expeditions.

Cruise-RV	Device	Enviroment	Station	Environmental samples	Sampling depth (m)	Latitude (°S)	Longitude (°w)	Date	Reference
HADES SONNE SO-261	Multi--corer (MUC)	Hadal sediments	A10	Hadal sediments (0-1, 1-2 and 2-3 cm)	7734	20.32	71.29	26/03/2018	This study
			A4	Hadal sediments (0-1, 1-2 and 2-3 cm)	7890	23.81	71.37	11/03/2018	
			A5	Hadal sediments (0-1, 1-2 and 2-3 cm)	8063	23.36	71.34	14/03/2018	
ChiMeBo SONNE SO-211	Multi--corer (MUC)	Bathyal Sediments	B12	Upper bathyal sediment (0-1 cm)	529	23.59	70.67	02-29/11/2010	This study
			B08	Upper bathyal sediment (0-1 cm)	539	25.2	70.68	02-29/11/2010	
			B22	Upper bathyal sediment (0-1 cm)	545	27.29	71.05	02-29/11/2010	
			B07	Lower bathyal sediment (0-1 cm)	920	25.07	70.66	02-29/11/2010	
			B05	Lower bathyal sediment (0-1 cm)	957	27.5	71.13	02-29/11/2010	
			B11	Lower bathyal sediment (0-1 cm)	1113	23.85	70.65	02-29/11/2010	
			B04	Lower bathyal sediment (0-1 cm)	1200	27.45	71.16	02-29/11/2010	
LowpHOX-2 Cabo de Hornos	Rosette (Niskin bottles)	Water column	T3/T5	Chlorophyll maximun (0.3-2.7 µm)	9-10	20.07/20.03	70.36/70.89	04-06/02/2018	Cantarero et al., 2020
			T3/T5	Upper chemocline (0.3-2.7 µm)	25-28	20.07/20.03	70.36/70.89	04-06/02/2018	
			T3/T5	Lower chomocline (0.3-2.7 µm)	35-45	20.07/20.03	70.36/70.89	04-06/02/2018	
			T3/T5	Upper OMZ (0.3-2.7 µm)	55-60	20.07/20.03	70.36/70.89	04-06/02/2018	
			T3/T5	Core OMZ (0.3-2.7 µm)	250	20.07/20.03	70.36/70.89	04-06/02/2018	
			T3/T5	Mesopelagic zone (0.3-2.7 µm)	750	20.07/20.03	70.36/70.89	04-06/02/2018	

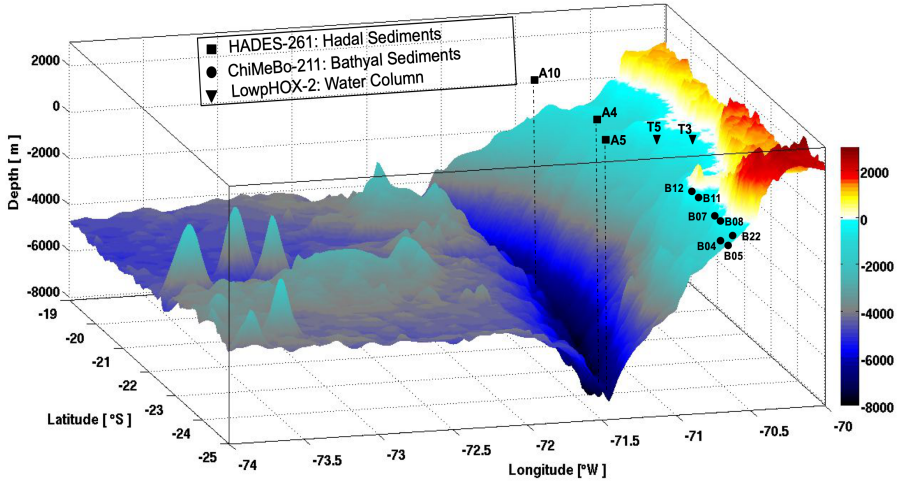

Figure 1. Three-dimensional map of the Atacama Trench showing the sampling locations of this study. The black squares indicate the hadal sediment sampling stations, the black circles indicate the bathyal sediment sampling stations from Matys et al. (2017), and the black triangles indicate water column sampling stations from Cantarero et al. (2020).

https://doi.org/10.5194/bg-2021-232
Preprint. Discussion started: 3 September 2021

Surface sediments from the bathyal (0-1 cm) and the hadal AT region (0-1 cm, 1-2 cm and 2-3 cm) were collected using a multi-corer (MUC) equipped with twelve 60-cm-long acrylic tubes (6-10 cm diameter for bathyal sediments and 9.5 cm diameter for hadal sediments). During the HADES expedition, an autonomous lander equipped with a Seabird SBE-19 plus CTD and 2 Niskin bottles (30 L) was used to obtain hydrographic data down to ~7850 m (SO261 cruise). Hadal sediments from the HADES-SO261 cruise were cold-stored after the sampling, and during their transit to the University of Bremen and then to the University of Colorado Boulder. Information about the sampling of bathyal sediments during the ChiMeBo-SO211 cruise can be found in Matys et al. (2017). All samples were processed, extracted, and analyzed in the Organic Geochemistry Laboratory at the University of Colorado Boulder as described below.

We compare our IPL results from surface sediment in the hadal and bathyal regions against samples from the overlying water column from the LowPhOx-2 cruise recently reported by Cantarero et al. (2020). This includes size-fractionated suspended organic matter (0.3-2.7 µm and 2.7-53 µm) at two stations and from six water depths that are representative of the dominant biogeochemical zonation associated with the OMZ of this region: chlorophyll maximum (~10 m), upper chemocline (~25 m), lower chemocline (~45 m), upper OMZ (~60 m), core OMZ (~250 m), and mesopelagic zone (~750 m) (See Table 1 and Cantarero et al., 2020 for further details).

2.2. Analytical methods

2.2.1 Lipid extraction

Sediment samples from the AT were freeze dried before extraction. Approximately 1-2 grams of dry sediment was placed in a combusted glass centrifuge tube and extracted using a modified version (Wörmer et al., 2013) of the Bligh and Dyer Extraction method (Bligh and Dyer, 1959) as detailed in Cantarero et al. (2020). Briefly, before extraction, we added 1 µg of C16 PAF ($C_{26}H_{54}NO_7P$) to each sample as an internal standard. Samples were sequentially extracted using Dichloromethane:MeOH:Phosphate buffer (1:2:0.8 v:v:v; 2x), Dichloromethane:MeOH:Trichloroacetic buffer (1:2:0.8 v:v:v; 2x) and Dichloromethane:MeOH (1:5 v:v; 1x). After each addition, samples were vortexed for 30 seconds, sonicated for 10 minutes, and then centrifuged for 5 minutes at 2000 rpm. Each extraction was then transferred to a separatory funnel where a total lipid extract (TLE) was combined and then concentrated under a gentle N_2 stream. Before analysis, the TLEs were resuspended in Dichloromethane:Methanol (9:1) v/v and filtered through a 0.45 µm polytetrafluoroethylene (PTFE) syringe filter. The processing and extraction of bathyal sediments from the ChiMeBo-SO211 cruise and water column samples from the LowpHOx-2 cruise has been reported by Matys et al. (2017) and Cantarero et al. (2020), respectively. TLEs were transferred into 2 ml vials with 200 µl inserts, and dissolved in 100 µl of Dichloromethane:MeOH [9:1, v:v].

2.2.2. IPL analysis

IPL were analyzed according to Wörmer et al. (2013) and as described in Cantarero et al. (2020) using a Thermo Scientific Ultimate 3000 High Performance Liquid Chromatograph (HPLC) coupled to a Q Exactive Focus Orbitrap-Quadrupole High Resolution Mass Spectrometer (HPLC-HRMS) via electrospray ionization (ESI). The HPLC program comprised a flow rate of 0.4 mL/min using a mixture of two mobile phases: mixture A consisted

https://doi.org/10.5194/bg-2021-232
Preprint. Discussion started: 3 September 2021

of Acetonitrile:Dichloromethane (75:25, v:v) with 0.01% formic acid and 0.01% NH_4OH; mixture B consisted of Methanol:H_2O (50:50, v:v) with 0.4% formic acid and 0.4% NH_4OH. We used a linear gradient as follows: 1% B (0–2.5 min), 5% (4 min), 25% B (22.5 min), 40% B (26.5 min–27.5 min), and the HPLC column was kept at 40 °C. Samples were injected (10 µl) dissolved in Dichloromethane:Methanol (9:1, v:v).
ESI settings comprised: sheath gas (N_2) pressure 35 (arbitrary units), auxiliary gas (N_2) pressure 13 (arbitrary units), spray voltage 3.5 kV (positive ion ESI), capillary temperature 265°C, S-Lens RF level 55 (arbitrary units). The instrument was calibrated for mass resolution and accuracy using the Thermo Scientific Pierce LTQ Velos ESI Positive Ion Calibration Solution (containing a mixture of caffeine, MRFA, Ultramark 1621, and N-butylamine in an acetonitrile/methanol/acetic acid solution).

IPLs were identified on positive ionization, on both full scan and data depended MS^2, based on their molecular weights as either protonated $(M + H)^+$ or ammonium $(M + NH_4)^+$ adducts compounds, fragmentation patterns, and retention times, and as compared against relevant literature (Sturt et al., 2004; Schubotz et al., 2009a; Wakeham et al., 2012) and the internal database of the Organic Geochemistry Lab at CU Boulder.

The peak areas of individual IPLs were integrated using the Thermo Fisher Scientific TraceFinder software using extracted ion chromatograms of their characteristic molecular ions. IPL abundances were determined with a combination of an internal standard (C_{16}PAF, Avanti Lipids) for recovery estimates and an external calibration to a linear regression between peak areas and known concentrations of an IPL cocktail comprised of 17 different IPL classes across a 5-point dilution series (0.001–2.5 ng/µl) (see Cantarero et al., 2020). Deuterated standards (Avanti Lipids: d7-PC, d7-PG, d7-PE and d9-DGTS) were used to correct for potential matrix effects on ionization efficiency. The relative response factors followed the order: MGDG >DGTS>DGTA >PDME >PME >PG > PC> PE >SQDG > DGCC > DGDG. Lipids classes were grouped into phospholipids (PG; phosphatidylglycerol, PE; phosphatidylethanolamine, PC; phosphatidylcholine, and PME/PDME; Phosphatidyl(di)methylethanolamine); glycolipids (MG; Monoglycosyldiacylglycerol, DG; Diglycosyldiacylglycerol, and SQ; Sulfoquinovosyldiacylglycerol), Betaine lipids (DGTA; Diacylglyceryl hydroxymethyl-trimethyl-β-alanine, DGTS; Diacylglyceryl trimethylhomoserine, and DGCC; Diacylglycerylcarboxy-N-hydroxymethyl-choline) and Other lipids (Gly-Cer; Glycosidic ceramides, PI; phosphatidylinositol, and OL; Ornithine lipids).

2.3. Statistical analyses

We used the Bray–Curtis similarity coefficient (Mirzaei et al., 2008) to produce hierarchical clustering of the abundance of classes and molecules of IPLs, two types of p-values were available: approximately unbiased (AU) p-value and bootstrap probability (BP) value with the number of bootstrap replications of 10,000 (Suzuki and Shimodaira, 2006). We performed non-metric Multidimensional Scaling (NMDS) (Warton et al., 2012) to examine the dissimilarity between the IPLs in each sample. The calculated distances to group centroids were based on Bray-Curtis dissimilarity from IPLs abundances matrix, and the significance of the associations was determined by 999 random permutations. Significance tests of the multivariate dissimilarity between groups were made using Analysis of Similarity (ANOSIM), where complete separation and no separation among groups is suggested by R = 1 and R = 0, respectively (Clarke and Gorley, 2015). Statistical differences in the numbers of carbon atoms and double bonds were identified by ANOVA and Tukey's HSD (honestly significant difference) post hoc test. We used similarity of percentage (SIMPER) analysis to identify the percentage contributions of IPLs which accounted

https://doi.org/10.5194/bg-2021-232
Preprint. Discussion started: 3 September 2021


Biogeosciences Discussions Open Access EGU

for > 90% of the similarity within each cluster. The multivariate statistical analyzes, as well as other statistical analyses were calculated using the Vegan package (Oksanen et al., 2013) of open-source software R version 3.6.2 within the ggplots package (Warnes et al., 2015).

3. Results

3.1 Hydrographic conditions

The potential temperature-salinity-dissolved oxygen (θ-s-O_2) diagrams revealed an oxygenated and well-mixed water mass occupying the deeper parts of the AT (Fig. S1). However, the upper 1000 m shows variability in temperature (12-23 °C), salinity (34.4 - 34.8) and oxygen (0.5-267 µM). In the mesopelagic and bathypelagic zone of AT between 1000 and 4000 m, more stable physical-chemical conditions are apparent (temperature ~ 2.3 °C, salinity ~34.6, oxygen ~120.6 µM). Below 4000 m, average conditions were characterized by a potential temperature ~1.8 ° C, salinity ~34.7, and oxygen ~143 µM (Fig. S1). A physical-chemical characterization of the water column during the ChiMeBo-SO211, LowpHOx-2, and HADES-SO261 cruises has been reported in Matys et al. (2017), Cantarero et al. (2020) and Vargas et al. (2021), and Fernández-Urruzola et al. (2021), respectively.

3.2 IPLs in surface sediments of the Atacama trench

3.2.1. Distribution of IPL classes by polar head groups

The 16 sediment samples from bathyal and hadal regions statistically grouped into four clusters based on their dominant polar head group classes (Fig. 2, chemical structures in Fig. S2). Clusters 1 and 2 had approximately unbiased (AU) p-values of 91% and 88%, respectively. Cluster 3 had the highest AU p-value of ≥ 97%, whereas Cluster 4 had the lowest AU p-value of 61%. The cluster analysis revealed a degree of spatial heterogeneity between bathyal and hadal depths and between the top three centimeters of hadal sediments, which results in the lack of a clear separation between hadal and bathyal environments. In addition, the 0-1 cm hadal sediments at A4 station were un-clustered, consistent with a distinct distribution pattern of IPL classes.

Cluster 1, composed of only hadal samples from three different stations and depths, included phospholipids as the most abundant IPL class (Fig. 2). Clusters 2, 3 and 4, composed of mixed bathyal and hadal samples, were mostly differentiated by changes in the relative abundances of non-phosphorous IPLs including betaine classes. The un-clustered sample was characterized by the lowest relative abundance of phospholipids and the highest relative abundance of betaine lipids (especially DGCC).

https://doi.org/10.5194/bg-2021-232
Preprint. Discussion started: 3 September 2021

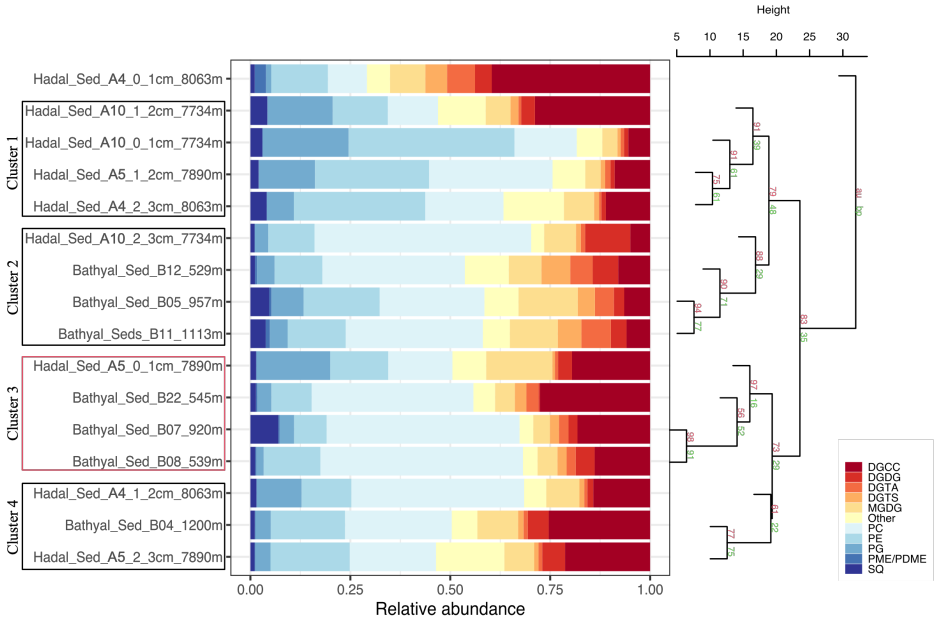

Figure 2. Cumulative bar charts of the fractional abundance of IPL classes in each surface sediment sample from the bathyal and hadal regions (left panel). Samples were grouped according to arithmetic mean (UPGMA) hierarchical clustering based on Euclidean distances. The p-values are shown at branches, approximately unbiased (AU) in red and bootstrap probability (BP) in green (right panel). Clusters 3 with an AU ≥ 95% confidence are indicated by the red rectangles (left) and are considered to be strongly supported by the data.

3.2.2. Distribution of individual IPLs

An overview of the most important IPLs contributing to dissimilarity between samples (Fig. 3) was obtained through a SIMPER analysis based on Bray-Curtis coefficient within each cluster. Samples in Cluster 1 were on average 59.5% similar, with 14 individual IPLs contributing 50.6% of the total similarity. This cluster exhibited a high contribution of PE (32:1, 33:1, and 34:2), PG (36:2), and DGCC (26:0, 27:0 and 28:0) molecules (Table 2). Additionally, this cluster exhibited a large diversity of PC molecules, with lower relative abundance (Fig. 3). Samples in Cluster 2, on the other hand, which includes mainly bathyal stations, were on average 58.8% similar and exhibited a high contribution of PC (35:0, 32:1, 36:2, 33:1, and 35:1) (Table 2). While this cluster shows a wide range of molecules, including PG, PE and MGDG, their relative contributions are low (Fig. 3). Samples in Cluster 3 were on average 57.3% similar and included three bathyal and one hadal stations. This cluster exhibited a high contribution of DGCC (42:6) and PC (35:0, 33:2, 30:1, and 29:2) molecules (Table 2). Samples in Cluster 4 were on average 63.6% similar, and exhibited a high contribution of PC (30:2, 33:2), DGCC (42:6), MGDG (28:0), and PE (33:2 and 31:2) molecules (Table 2). The un-cluster sample (Hadal sediment of 0-1 cm at A4 station) is mainly composed by the DGCC 42:6 (Fig. 3). In general, phospholipids showed a wide distribution and were found across all sediment samples. The total dissimilarity between Clusters 1 and 2 was 59.17%, with PC 35:0, PE 32:1, PI-AR, PG 36:2, DGCC 27:0, PC 36:2, PC 34:1, PC 32:1, DGCC 26:0, and PC 35:1 contributing 32.4% of it (Table 2). The total dissimilarity between Clusters 1 and 3 was 60.7%, with DGCC 42:6, PC 35:0, PI-AR, PE 32:1, PG 36:2, DGCC 27:0 and 26:0, and PC 33:2 contributing 38.1% of it (Table 2). The total

https://doi.org/10.5194/bg-2021-232
Preprint. Discussion started: 3 September 2021

dissimilarity between Clusters 1 and 4 was 62.5%, with DGCC 42:6, PC 30:2, PE 32:1, PC 35:0, PG 36:2, PC 33:2, and DGCC 27:0 contributing 37.62% of it (Table 2).

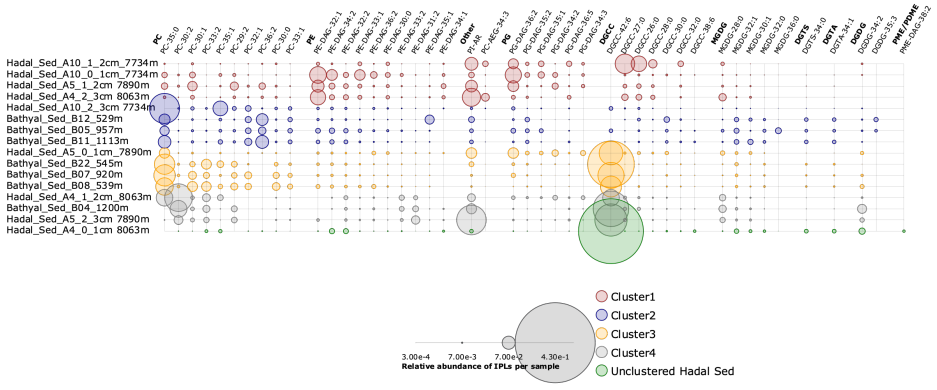

Figure 3. Relative abundance of individual IPLs contributing most of the dissimilarity between the 4 clusters shown in Fig. 2. Sampling stations were organized from top to bottom and are shown using the same order from hierarchical clusters in Fig. 2, and were organized from left to right by IPL classes. The circle ratios are proportional to the relative abundance of IPLs in each sample (bottom panel).

https://doi.org/10.5194/bg-2021-232
Preprint. Discussion started: 3 September 2021

Biogeosciences Discussions Open Access EGU

Table 2. SIMPER (similarity percentage) analysis. Average abundance and contribution of IPLs that explain the main differences among the sediment sampling stations is based on the hierarchical clusters shown in Fig. 2.

Group Cluster 1 Cluster 1: Average Similarity = 59.53					
IPLs	Average Cluster 1	Average Similarity	Similarity/SD	Contribution (%)	Cumulative (%)
PI-AR	0.06	4.76	2.46	7.99	7.99
PE-DAG-32:1	0.06	4.37	1.45	7.34	15.33
PG-DAG-36:2	0.05	3.79	2	6.36	21.69
PE-DAG-33:1	0.03	2.06	33.49	3.45	25.14
PE-DAG-34:2	0.03	1.89	1.74	3.17	28.31
DGCC-26:0	0.04	1.84	2.04	3.09	31.4
PC-30:1	0.03	1.76	2.21	2.96	34.36
DGCC-27:0	0.04	1.74	1.8	2.93	37.3
PE-DAG-30:0	0.02	1.7	13.1	2.86	40.15
PE-DAG-32:2	0.02	1.39	1.07	2.34	42.49
PC-35:0	0.02	1.31	1.52	2.2	44.69
DGCC-28:0	0.02	1.22	1.96	2.05	46.74
PC-26:0	0.02	1.18	1.46	1.99	48.73
PC-28:0	0.02	1.14	1.59	1.91	50.63
Group Cluster 2 Cluster 2: Average Similarity = 58.79					
IPLs	Average Cluster 2	Average Similarity	Similarity/SD	Contribution (%)	Cumulative (%)
PC-35:0	0.08	5.63	7.54	9.58	9.58
PC-32:1	0.03	3.12	31.24	5.3	14.88
PC-36:2	0.05	2.74	1.13	4.67	19.55
PC-33:1	0.02	2.04	10.17	3.46	23.01
PC-35:1	0.03	1.63	4.48	2.77	25.78
PI-AR	0.02	1.61	3.9	2.74	28.53
MGDG-32:1	0.02	1.44	1.35	2.45	30.98
PE-DAG-32:1	0.02	1.38	5.03	2.35	33.33
PE-DAG-34:2	0.02	1.38	2.75	2.35	35.68
PE-DAG-32:2	0.02	1.22	2.79	2.08	37.76
PC-32:0	0.01	1.14	5.69	1.94	39.69
PG-DAG-36:2	0.02	1.1	3.23	1.87	41.57
PG-DAG-35:2	0.02	1.09	1.23	1.86	43.43
PC-34:1	0.04	1.06	0.41	1.8	45.23
PC-30:1	0.01	1.05	7.23	1.79	47.02
PC-32:2	0.01	0.95	11.7	1.61	48.64
PC-29:2	0.01	0.95	2.69	1.61	50.25
Group Cluster 3 Cluster 3: Average Similarity = 57.31					
IPLs	Average Cluster 3	Average Similarity	Similarity/SD	Contribution (%)	Cumulative (%)
DGCC-42:6	0.16	12.84	6.72	22.4	22.4
PC-35:0	0.08	4.78	1.14	8.33	30.74
PC-33:2	0.03	2.07	1.19	3.61	34.35
PC-30:1	0.03	1.96	1.82	3.42	37.77
PC-29:2	0.03	1.79	1.2	3.12	40.89
PI-AR	0.05	1.69	1.09	2.95	43.84
MGDG-32:1	0.01	1.22	7.66	2.14	45.98
PE-DAG-32:1	0.01	1.18	10.45	2.05	48.03
PC-30:0	0.02	1.13	1.22	1.97	50
Group Cluster 4 Cluster 4: Average Similarity = 63.64					
IPLs	Average Cluster 2	Average Similarity	Similarity/SD	Contribution (%)	Cumulative (%)
PC-30:2	0.12	9.04		14.21	14.21
DGCC-42:6	0.14	8.91		13.99	28.2
PI-AR	0.05	4.14		6.5	34.71
PC-33:2	0.04	3.71		5.83	40.54
MGDG-28:0	0.04	3.44		5.41	45.95
PE-DAG-33:2	0.03	2.52		3.97	49.92
PE-DAG-31:2	0.03	2.14		3.37	53.28

Groups Cluster 1 & Cluster 2 Average dissimilarity = 59.17						
IPLs	Average Cluster 1	Average Cluster 2	Average Dissimilarity	Dissimilarity/SD	Contribution (%)	Cumulative (%)
PC-35:0	0.02	0.08	3.18	1.34	5.37	5.37
PE-DAG-32:1	0.06	0.02	2.35	1.73	3.98	9.35
PI-AR	0.06	0.02	2.21	1.74	3.73	13.08
PG-DAG-36:2	0.05	0.02	1.98	1.64	3.35	16.43
DGCC-27:0	0.04	0	1.93	1	3.26	19.69
PC-36:2	0.01	0.05	1.79	1.57	3.02	22.71
PC-34:1	0	0.04	1.79	1.03	3.02	25.73
PC-32:1	0.01	0.03	1.36	5.58	2.3	28.03
DGCC-26:0	0.04	0.01	1.34	0.95	2.27	30.3
PC-35:1	0.01	0.03	1.27	0.9	2.15	32.45
PE-DAG-33:1	0.03	0.01	1.02	1.2	1.73	34.18
PC-33:1	0	0.02	0.96	7.61	1.63	35.8
DGCC-28:0	0.02	0	0.93	1.28	1.57	37.37
PC-AEG-34:3	0.02	0	0.9	1.03	1.52	38.89
PE-DAG-34:2	0.03	0.02	0.88	1.2	1.49	40.38
MGDG-32:1	0	0.02	0.83	1.81	1.4	41.78
PC-30:1	0.03	0.01	0.83	1.15	1.4	43.18
PG-DAG-34:2	0.02	0	0.77	1.05	1.3	44.48
PE-DAG-33:0	0.02	0	0.76	1.11	1.29	45.77
PG-DAG-35:1	0.02	0.01	0.74	1.22	1.26	47.03
PE-DAG-34:1	0.02	0	0.74	2.06	1.25	48.27
PC-26:0	0.02	0	0.72	1.74	1.21	49.48
DGCC-30:0	0	0.01	0.68	1.32	1.15	50.64
Groups Cluster 1 & Cluster 3 Average dissimilarity = 60.69						
IPLs	Average Cluster 1	Average Cluster 3	Average Dissimilarity	Dissimilarity/SD	Contribution (%)	Cumulative (%)
DGCC-42:6	0	0.16	8.02	3.2	13.21	13.21
PC-35:0	0.02	0.08	3.05	1.87	5.02	18.23
PI-AR	0.06	0.05	2.66	1.6	4.39	22.62
PE-DAG-32:1	0.06	0.01	2.49	1.74	4.1	26.72
PG-DAG-36:2	0.05	0.02	1.9	1.49	3.14	29.86
DGCC-27:0	0.04	0.01	1.84	0.97	3.03	32.89
DGCC-26:0	0.04	0.01	1.59	1.12	2.62	35.52
PC-33:2	0	0.03	1.58	1.7	2.61	38.12
PE-DAG-34:2	0.03	0.01	1.13	1.35	1.86	39.98
PE-DAG-33:1	0.03	0.01	1.07	1.33	1.76	41.75
PC-AEG-34:3	0.02	0	0.95	1.08	1.57	43.31
PC-29:2	0.02	0.03	0.95	1.88	1.56	44.87
DGCC-28:0	0.02	0	0.9	1.25	1.49	46.36
PC-30:1	0.03	0.03	0.87	1.35	1.43	47.79
PE-DAG-33:0	0.02	0	0.76	1.07	1.26	49.05
PG-DAG-34:2	0.02	0.01	0.76	1.1	1.26	50.3
Groups Cluster 1 & Cluster 4 Average dissimilarity = 62.47						
IPLs	Average Cluster 1	Average Cluster 4	Average Dissimilarity	Dissimilarity/SD	Contribution (%)	Cumulative (%)
DGCC-42:6	0	0.14	6.99	2.57	11.19	11.19
PC-30:2	0.01	0.12	5.66	3.64	9.06	20.24
PE-DAG-32:1	0.06	0	3.17	2.09	5.07	25.31
PC-35:0	0.02	0.04	2.22	1.6	3.55	28.86
PG-DAG-36:2	0.05	0.01	2.12	1.64	3.4	32.27
PC-33:2	0	0.04	1.9	15.16	3.04	35.3
DGCC-27:0	0.04	0.02	1.45	0.78	2.32	37.62
PE-DAG-34:2	0.03	0	1.35	1.44	2.16	39.78
PI-AR	0.06	0.05	1.3	1.6	2.08	41.86
DGCC-26:0	0.04	0.01	1.26	0.89	2.02	43.88
DGDG-34:2	0	0.03	1.25	1.17	2	45.88
PE-DAG-31:2	0	0.03	1.21	4.58	1.93	47.81
PE-DAG-33:1	0.03	0.01	1.2	1.46	1.92	49.73
PE-DAG-33:3	0	0.02	1.16	4.61	1.86	51.59

https://doi.org/10.5194/bg-2021-232
Preprint. Discussion started: 3 September 2021

340 **3.3 Distribution of alkyl chains based on length and degree of unsaturation**
341
342 The difference in the total number of acyl carbon atoms in both alkyl chains, rather than in individual fatty acids,
343 and in the number of acyl double bonds within each cluster is shown in Fig. 4. Statistical differences of IPLs
344 classes within each cluster was obtained through a Tukey HSD post-hoc test at a significant level of $p<0.05$ (Fig.
345 4a, b). The average number of carbon atoms in the diglyceride moieties of IPLs in the Cluster 1 showed that
346 DGCC, MGDG, Others, PC, and PG were all distinct from one another ($n = 283$; $P < 0.05$; Fig. 4a). PG and Others
347 were characterized by relatively long alkyl chains (35-36 C atoms, respectively) and DGCC for shorter alkyl
348 chains (32 C atoms). In general, Cluster 1 exhibited a wide range of chain lengths among diacylglycerols (DAGs)
349 (28-36 C atoms). Cluster 2 showed narrower ranges than Cluster 1 (30-36 C atoms). This cluster also showed no
350 statistical difference ($p > 0.05$) among IPL classes (Fig. 4a), following pairwise comparisons with Tukey's HSD
351 post-hoc test, despite the wide range of DGCC structures. Cluster 3, while it exhibited low variability in betaine
352 lipids, showed the highest number of carbon atoms in DGCCs (42). On the contrary, Cluster 4 showed high
353 viability in DGCCs, which did not exceed 42 carbon atoms. Within the phospholipid class, PG showed the highest
354 number of carbon atoms in all clusters, the mean we observed was 34 carbon atoms and a range of 32 to 37 (Fig.
355 4a). The un-cluster sample (hadal sediment of 0-1 cm at A4 station) was characterized by relatively longer alkyl
356 chains (up to 42 C atoms) than Cluster 1 (Fig. 4a).
357
358 Overall, the degree of unsaturation (i.e., number of double bounds) within clusters was variable (Fig. 4b). Cluster
359 1 predominantly consisted of fully saturated and mono-unsaturated IPLs, except for PG that showed 2 double
360 bonds in average. In Cluster 2, the fatty acids of DGCCs were distinctly variable, although they exhibited 2
361 unsaturations on average. A similar pattern was observed in DGDGs with an average of 2.5 unsaturations (Fig.
362 4b). DGTS, MGDGD, PC and SQ showed non to 1 unsaturation, whereas DGTA, PE and PG exhibited between
363 1 and 2.5 unsaturations. Cluster 3 showed more than 5 unsaturations on average for DGCC, unlike other IPL
364 classes that did not exceed 2 unsaturations. In Cluster 4, PG and DGCC presented ~3 and ~5 unsaturations on
365 average. Also, on average, DGDG and SQ exhibited 2 unsaturations, MGDG and Others were mono-unsaturated,
366 and DGTS were saturated (Fig. 4b). Additionally, the ratio of total unsaturated fatty acids to total saturated fatty
367 acids in IPLs increased from (on average) ~0.9 in all water column samples (pressure range of 2-76 Bars) to ~2.7
368 in the bathyal (pressure range of 54-113 Bars) and hadal sediments (pressure range 777-810 Bars) (Fig. 5).

https://doi.org/10.5194/bg-2021-232
Preprint. Discussion started: 3 September 2021

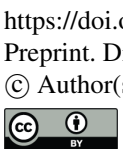

Biogeosciences
Discussions
Open Access
EGU

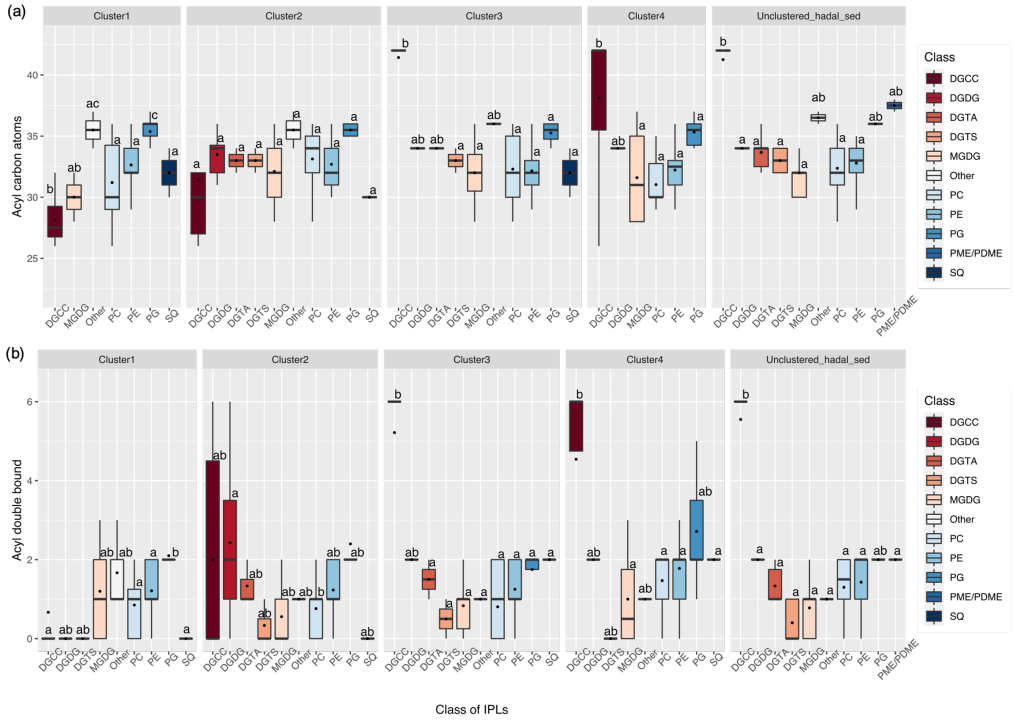

Figure 4. Total number of acyl carbon atoms (a) and acyl double bonds (b) in IPL classes across the distinct clusters shown in Fig. 2. The letters "a" and "b" in the plots indicate the presence of statistically distinct groups ($p < 0.05$) from both ANOVA and post-hoc Tukey HSD tests, respectively.

https://doi.org/10.5194/bg-2021-232
Preprint. Discussion started: 3 September 2021

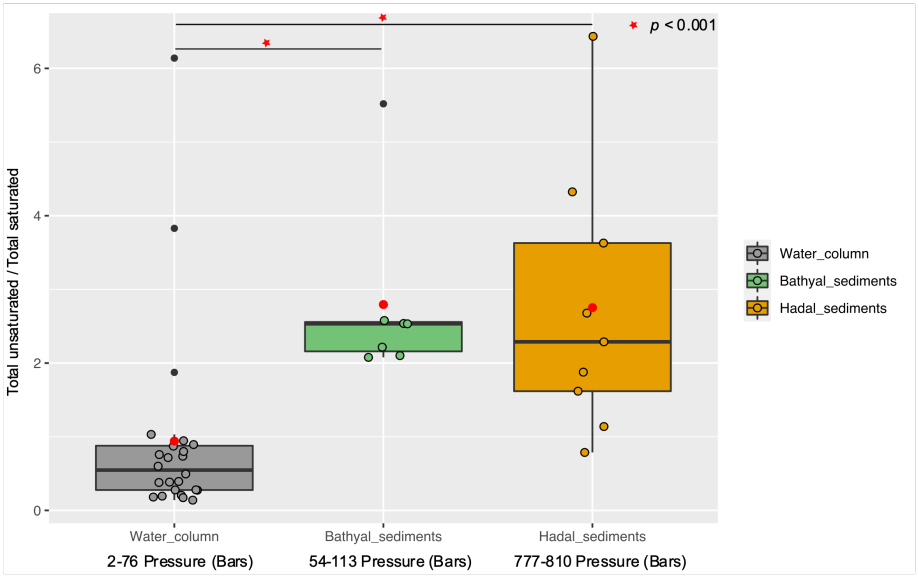

Figure 5. Boxplot showing difference in ratio of total unsaturated fatty acids to total saturated fatty acids derived from IPL across water column (Cantarero et al., 2020) and sediments of Atacama Trench (this study). The average in each environment were shown in red circles and Wilcoxon test (p-value < 0.001) shows that the sediments have statistical ratios higher than the water column.

3.4 Unique IPLs in hadal sediments of the Atacama Trench

To test whether IPLs detected in the Atacama Trench (AT) exhibit signals unique to this environment, we compared our results against IPL data from the overlying water column (top 750 meters) recently reported by Cantarero et al. (2020). Water-column particles and bathyal-hadal sediments shared 242 (96.1%) IPL structures (Fig. 6a), while hadal sediments and water-column particles shared 14 (0.02%), and hadal and bathyal sediments shared 55 (3.6%). Of all the analyzed IPLs reported in this study, eight of them were unique to the Atacama Trench sediments and not present in shallower sediments nor the overlying water column. They include five glycolipids (SQDG-42:11, SQDG-23:0, DGDG-35:1, DGDG-35:2 and DGDG-37:1), two phosphatidyl-inositols (PI-diOH-Ext-AR and PI-OH-AR), and one ornithine lipid (OL-37:6). While unique to hadal sediments, their total concentration was low (~53.32 ng g^{-1} sediment) and they contributed ~0.00012% of the total IPL pool (Fig. 6a). We then performed a cluster analysis to compare IPLs in deep-sea surface sediments against IPLs reported in the overlying water column (Cantarero et al., 2020; Fig. 6b). Cluster 1 comprised samples from the core OMZ in the free-living fraction (AU p-value of 100%). Cluster 2 comprised samples from both the upper and lower oxyclines (~14-60 m) as well as from the chlorophyll maximum (AU p-value of 99%). Cluster 3 comprised bathyal and hadal samples (AU p-value of 99%). Cluster 4 mostly comprised the deepest water column sample (mesopelagic region at 750 m) and hadal samples (AU p-value of 98%; Fig. 6b). We also compared IPLs in hadal and bathyal sediments against the pool of IPLs reported as diagnostic of the planktonic community inhabiting the chlorophyll maximum in the upper water column (Cantarero et al., 2020), and thus assess their export and stability through

https://doi.org/10.5194/bg-2021-232
Preprint. Discussion started: 3 September 2021

their transit to the deep-sea. Notably, these IPLs only represent ~0.001-0.005% and 0.002-0.03% of the total IPL pool in hadal and bathyal sediments, respectively (Fig. S3).

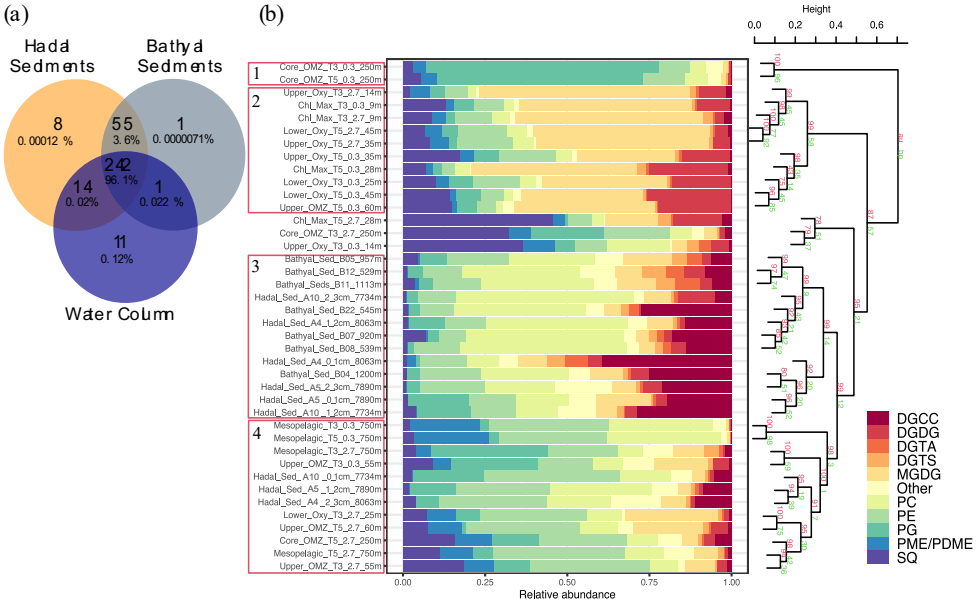

Figure 6. Comparison of IPLs in sediments (this study) and the overlying water column (Cantarero et al., 2020). (a) Venn diagram showing unique and shared IPL molecules in hadal and bathyal sediments and the water column. (b) Cumulative bar charts of IPL fractional abundances in each sampling station. Samples were grouped according to arithmetic mean (UPGMA) hierarchical clustering based on Euclidean distances. The cluster analysis on the right-hand size shows approximately unbiased (AU) and bootstrap probability (BP) in red and green numbers, respectively, as well as p-values are shown at branching points. Clusters with AU ≥ 95% confidence are highlighted in red on the left-hand side.

In sediments within the AT, we found a high degree of heterogeneity in total IPL concentrations among sites and different sediment levels (0–1, 1–2, 2–3 cm), which were an order of magnitude higher than bathyal sediments (see Figs. S4a, S4b). Hadal sediments at station A10 (7,734 m) showed a large range of phospholipid concentrations (~47–2,698 ng g^{-1} sediment) (supplementary Fig. S4b). Although the highest total IPL abundances were observed at hadal station A10 (Fig. S4b), the greatest diversity in IPL composition was observed in the 0-1 cm of the hadal station A4, previously referred to as un-clustered (see Fig. 2). The most abundant IPL class in hadal sediments were phospholipids, PCs (~41-2,698 ng g^{-1} sed.), PEs (~26-1,813 ng g^{-1} sed.) and PGs (5-937 ng g^{-1} sed). The concentration of IPLs normalized by TOC (ng IPL/g TOC) showed maximum values in the hadal station A10 (~150 ng IPL/g TOC), followed by lower values in the hadal stations A5 and A4 of ~50 and ~12 ng IPL/g TOC, respectively (Fig. S5).

https://doi.org/10.5194/bg-2021-232
Preprint. Discussion started: 3 September 2021

4. Discussion

4.1 Potential Biological Sources of IPLs

We evaluated the chemical characteristics and potential biological provenance of labile IPLs in the hadal zone of the AT as compared to the overlying water column and/or shallower bathyal sediments.

4.2 Potential sources of phospholipids

PG (Phosphatidylglycerol)

Phospholipids are common constituents of cellular membranes in most microorganisms (Ratledge and Wilkinson, 1988). Since PGs play an essential role in photosynthesis (Wada and Murata, 2007), they have therefore been mainly identified in algal and bacterial photoautotrophs (Dowhan, 1997; Sato et al., 2000; Gombos et al., 2002). However, their biological origin is highly diverse and also includes heterotrophic bacteria (Oliver and Colwell, 1973; Van Mooy et al., 2009; Popendorf et al., 2011b; Carini et al., 2015; Sebastián et al., 2016), methylotrophs (Batrakov and Nikitin, 1996), methanotrophic bacteria (Makula, 1978), *Pelagibacter ubique* (Van Mooy et al., 2009), and barophilic bacteria (e.g., DB21MT-2 and DB21MT-5) isolated from sediments from the Marianas Trench (Fang et al., 2000).

The hierarchical cluster analysis on variations in the relative abundance of PGs suggests that several compounds maintained a similar proportion in bathyal and hadal sediments, which differs from the water column (Fig. 7a). Most PGs in the bathyal and hadal sediments have long acyl carbon chains (C_{34}-C_{41}), and they show odd- and even-numbered polyunsaturated fatty acids (Fig. 7a). The average chain-lengths of even-numbered *n*-C_{18}, *n*-C_{20} and *n*-C_{22} fatty acids, mostly in PCs and PGs, are indicative of algal inputs (Kaneda, 1991; Thompson Jr, 1996; Bergé and Barnathan, 2005; Brandsma et al., 2012). However, since these PGs were not dominant in the water column, a source from deeper environments is likely. Specifically, PG-DAG-36:2, PG-DAG-35:2, PG-DAG-36:5, PG-DAG-37:2, and PG-DAG-41:4 are the dominant constituents of this IPL class in hadal-bathyal sediments (Fig. 7a). PG-DAG-36:2 has been described in surface waters of the North Sea and also detected in picoeukaryotes (Brandsma et al., 2012), and in heterotrophic bacteria in surface waters of the open South Pacific Ocean (Van Mooy and Fredricks, 2010). However, these PGs are not dominant in the water column near the Atacama Trench (Cantarero et al., 2020). On the other hand, PG-DAG-35:2, PG-DAG-36:5, PG-DAG-37:2 and PG-DAG-41:4 are not commonly reported in water-column studies. Thus, it is possible that PGs present in the AT sediments derive from *in situ* microbial production, and/or from the transport of labile organic matter present in surface sediment at shallower depths. PG-DAG-36:2 (Fig. 3) is the PG contributing most to the dissimilarity within the cluster containing only hadal sediments (Cluster 1 in Figure 2). Thus, this lipid appears to be more representative of *in situ* microbial production in this environment.

PE (Phosphatidylethanolamine)

PE and its methylated derivatives (PME, PDME) have been predominantly reported in membranes of diverse bacterial sources, including heterotrophic bacteria (Van Mooy and Fredricks, 2010; Schubotz et al., 2018a), nitrifying/denitrifying bacteria (Goldfine and Hagen, 1968), sulfate-reducing bacteria (Rütters et al., 2001; Sturt

https://doi.org/10.5194/bg-2021-232
Preprint. Discussion started: 3 September 2021


Biogeosciences Discussions Open Access EGU

et al., 2004), sulfur-oxidizing bacteria (Barridge and Shively, 1968; Imhoff, 1995; Wakeham et al., 2012), methanotrophic bacteria (Makula, 1978; Sturt et al., 2004), and barophilic bacteria (Fang et al., 2000).

PEs showed a similar distribution in bathyal and hadal sediments (Fig. 7b), where they are dominated by long-chain (C_{30-40}) polyunsaturated fatty acids, contrary to the shorter chains (C_{29-32}) of saturated and monounsaturated fatty acids present in the water column. PE-DAG-32:1, PE-DAG-32:2, and PE-DAG-33:1 are the dominant PE compounds of bathyal and hadal sediments. These IPLs have been previously reported in heterotrophic bacteria (Van Mooy and Fredricks, 2010; Brandsma et al., 2012). On the other hand, fatty acids in PEs including monounsaturated and polyunsaturated (e.g., $C_{20:5}$ and $C_{22:6}$) have been reported in barophilic bacteria isolated from sediments from the Marianas Trench (Fang et al., 2000). Thus, although we cannot confidentially rule out other sources, it is possible that PEs present in the AT sediments derive from *in situ* production by barophilic heterotrophic bacteria, and/or from the transport of labile organic matter from shallower water sediment. PE-DAG-32:1, PE-DAG-32:2 and PE-DAG-33:1 (Fig. 3) are the PEs that contributed most to the dissimilarity within the cluster containing only hadal sediment samples (Cluster 1 in Figure 2). Thus, this cluster appears to be representative of *in situ* microbial production in this environment.

PC (Phosphatidylcholine)

PCs were amongst the most diverse (43 structures: Fig. 7c) and abundant phospholipid class in hadal sediments (Fig. S4). PC is the major membrane-forming phospholipid in eukaryotes (Lechevalier, 1988; Sohlenkamp et al., 2003; Van Mooy et al., 2006; Van Mooy and Fredricks, 2010). Additionally, PC has been reported to be a major DAG in zooplankton, from protozoa to copepods and krill (Patton et al., 1972; Mayzaud et al., 1999; Lund and Chu, 2002). However, genomic data indicates that more than 10% of all bacteria possess the genetic machinery for PC biosynthesis (Sohlenkamp et al., 2003). PC has also been reported in nitrifying bacteria (Lam et al., 2007), photoheterotrophic bacteria (Koblížek et al., 2006; Van Mooy et al., 2006), and barophilic bacteria (Fang et al., 2000). In surface sediments of the Black Sea (2000 m), PCs were related to algal material rapidly exported from surface waters (Schubotz et al., 2009a).

Hadal and bathyal sediments, in addition to two OMZ core stations, were clustered in the PC class (AU p-value of 97%; Fig. 7c). This cluster showed PCs with long (C_{33-38}) and polyunsaturated fatty acids (up to 10 unsaturations). The dominant constituents were PC-35:0, PC-30:2, PC-30:1, PC-33:2, PC-35:1, PC-29:2, PC-32:1, and PC-36:2 (Fig. 7c). PC-36:2 and PC-30:1 has been associated with phytoplankton detritus (Schubotz et al., 2009a) and bacteria (Brandsma et al., 2012), whereas PC-32:1 has been associated with picoeukaryotes (Brandsma et al., 2012). Since the most abundant PCs in Cluster 1 have not been reported as dominant structures in any specific environment before, they are possibly produced *in situ* and/or derive from laterally transported sediment from shallower depths to the hadal region. Among bacteria, those membranes reported to contain PC belong to the alpha and gamma subgroups of the proteobacteria (Sohlenkamp et al., 2003). Given that these bacterial groups are abundant in trench samples from Puerto Rico (Eloe et al., 2011), the Mariana (Nunoura et al., 2015) and recently in the Atacama Trench (Schauberger et al., 2021), it is possible that PCs present in high abundance in the AT trenches is consistent with high abundance of proteobacteria in these regions. Given their general known

https://doi.org/10.5194/bg-2021-232
Preprint. Discussion started: 3 September 2021

association and abundance in AT sediments (Fig. S4), they likely derive primarily from bacterial sources and to a lesser extent from phytoplankton.

PME/PDME (Phosphatidyl(di)methylethanolamine)

PME/PDMEs have been observed in association with methanotrophic bacteria (Makula, 1978; Goldfine, 1984; Fang et al., 2000), sulfide oxidizer bacteria (Barridge and Shively, 1968), sulfate-reducing bacteria, mainly *Desulfobulbus spp* (Rossel et al., 2011), Proteobacteria (Oliver and Colwell, 1973; Goldfine, 1984), and barophilic bacteria from the Mariana Trench (Fang et al., 2000). Additionally, the occurrence of PME-DEG at some hadal stations suggests the presence of sulfate-reducing bacteria (Rütters et al., 2001; Sturt et al., 2004).

PME/PDMEs exhibited their lowest abundance (~10 ug g sed^{-1}) in sediment samples (Fig. S4b). In the bathyal and hadal sediments they were clustered (AU p-value of 97%) and dominated by PDME-DAG-33:1, PME-DAG-37:2, PME-DAG-34:2, PME-DAG-31:1, and PME-DEG-33:0 (Fig. S6a). PME-DEG-33:0 has been shown to correlate with high NO_2^- in the overlying water column of this area (Cantarero et al., 2020), which could suggest a potential association with denitrification processes. These structures have also been reported in the deep chemocline of the Cariaco basin (Wakeham et al., 2012), suggesting a potential chemoautotrophic and/or heterotrophic source. These signals are different from the water column, which is dominated by the saturated PME-32:0, PME-DAG-30:0, and PME-DAG-31:0 (Fig. S6a and S7; Cantarero et al., 2020). Thus, they most likely derive from *in situ* production and or/lateral transport rather than vertical export from the overlying water column. No particular PME/PDME were found to contribute to the dissimilarity between the cluster containing only hadal sediment samples (Cluster 1 in Figure 2) and other sediment samples.

https://doi.org/10.5194/bg-2021-232
Preprint. Discussion started: 3 September 2021

Biogeosciences
Discussions
Open Access
EGU

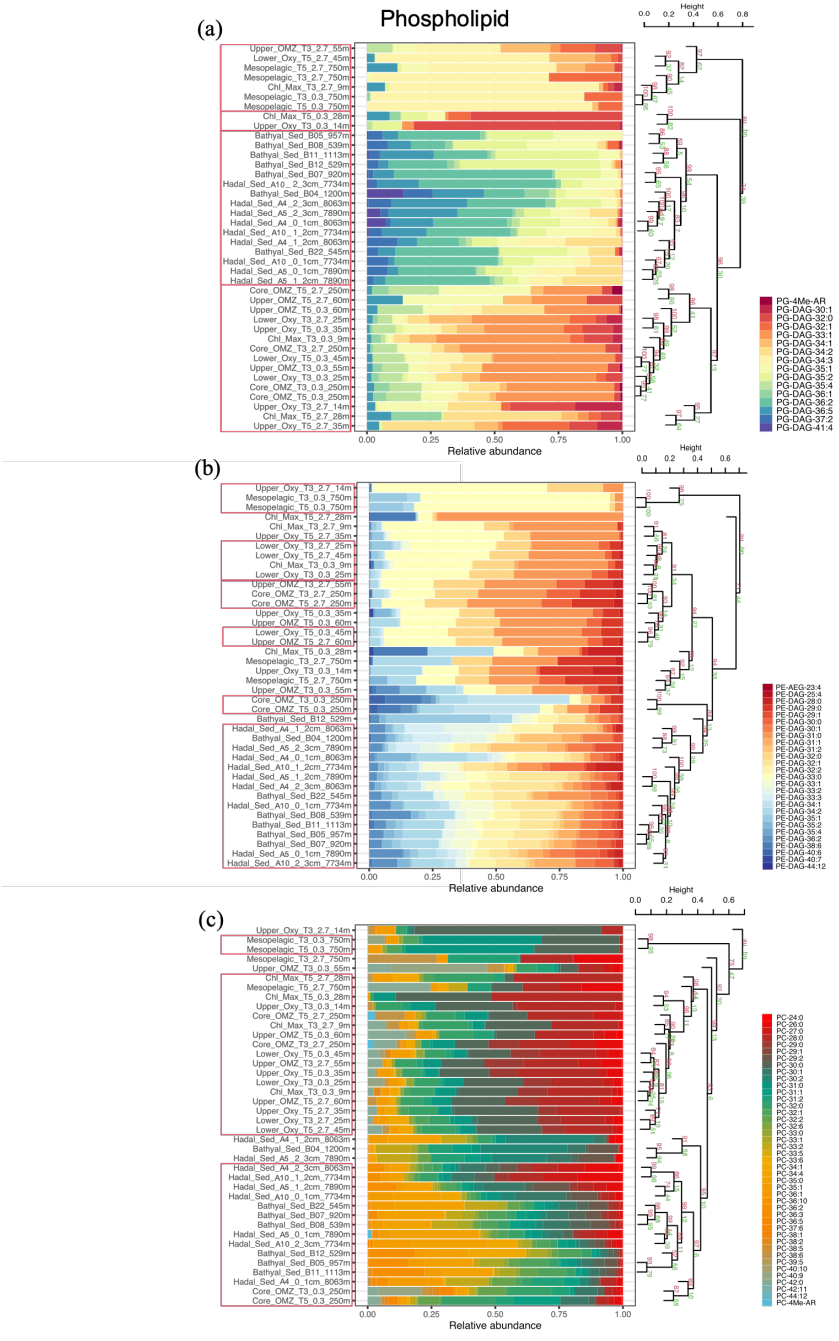

532

533 **Figure 7. Cumulative bar chart of phospholipid fractional abundances in all sample types. a) PG; b) PE; c) PC. The**
534 **number of carbon atoms and unsaturation in core fatty acids follow the order shown in the legend. The right panel**
535 **depicts a cluster analysis with approximately unbiased (AU) and bootstrap probability (BP) shown in red and green,**
536 **respectively, and p-values shown at branching points. The number of bootstrap replicates is 10000. Clusters with AU**
537 **≥ 95% confidence are highlighted in red boxes on the left-hand side.**

https://doi.org/10.5194/bg-2021-232
Preprint. Discussion started: 3 September 2021

538 **4.3 Potential sources of glycolipids**
539
540 **MGDG (Monoglycosyldiacylglycerol)**
541
542 Due to their dominant occurrence in chloroplast thylakoid membranes (Murata and Siegenthaler, 1998) and
543 particularly in cyanobacteria (Heinz, 1977; Harwood, 1998; Wada and Murata, 2007; Van Mooy and Fredricks,
544 2010), but also in heterotrophic bacteria (Popendorf et al., 2011b), MGDGs are probably the most abundant IPLs
545 on earth (Gounaris and Barber, 1983).
546 The hierarchical cluster groups of MGDGs in bathyal (AU p-value of 90%) and hadal (AU p-value of 98%)
547 sediments (Fig. 8a). The most abundant MGDGs in the bathyal and hadal sediments were MGDG-28:0, MGDG-
548 32:1, MGDG-30:1, MGDG-32:0 and MGDG-37:3. MGDG-28:0, and MGDG-30:1 are ubiquitous along the
549 oxycline of the overlying OMZ (Cantarero et al., 2020) and MGDG-32:1. MGDG-32:0 have been reported in
550 waters of the eastern south Pacific (Van Mooy and Fredricks, 2010). Thus, these MGDGs could indicate the
551 occurrence of at least some export of labile organic matter from surface waters in our study area. MGDG-37:3
552 does not appear to be a dominant structure in any specific environment previously reported, possibly being
553 produced *in situ* and /or laterally transported to hadal sediments.
554
555 **DGDG (Diglycosyldiacylglycerol)**
556
557 DGDGs are commonly found in membranes of eukaryotic algae and cyanobacteria (Wada and Murata, 1998;
558 Sakurai et al., 2006; Kalisch et al., 2016). DGDGs clustered together in bathyal and hadal sediments (AU p value
559 of 96%) whereas their distribution differed from the water column (Fig. 8b).
560 The most abundant DGDGs in hadal and bathyal sediments of the AT were DGDG-34:2, which has been
561 previously reported in Chlorophyta (da Costa et al., 2020), and DGDG-30:0, which is widely distributed in the
562 water column of this region (Cantarero et al., 2020). Thus, although they account for less than 10% of the total
563 IPL pool (Fig. 6b), their presence in bathyal and hadal sediments is likely indicating the occurrence of at least
564 some export of labile organic matter from surface waters.
565
566 **SQDG (Sulfoquinovosyldiacylglycerol)**
567
568 SQDG are predominantly produced by photoautotrophs (Van Mooy et al., 2006; Popendorf et al., 2011b),
569 including various groups of diatoms, brown and green algal chloroplast membranes (Harwood, 1998), and
570 cyanobacteria (Siegenthaler, 1998; Wada and Murata, 1998). SQDGs have also been found in bacteria from the
571 α- and γ-proteobacterial lineages (Benning, 1998). In the overlying water column of the Atacama Trench,
572 Cantarero et al., (2020) suggested a higher contribution of SQDGs from cyanobacteria than algae. Also, SQDGs
573 found in the deep Atlantic (down to ~4,000-5,000 m) appear to indicate a source and export from surface waters
574 (Gašparović et al., 2018).
575 SQDGs showed a consistent distribution in bathyal and hadal sediments, where they are dominated by long-chain
576 (C_{30-42}) fatty acids (Fig. 8c). This is contrasting to their distribution in the overlying water column where they are
577 dominated by shorter chains (C_{28-32}) of saturated fatty acids (Cantarero et al., 2020). SQDG-30:0, SQDG-32:0,
578 SQDG-30:2, and SQDG-38:4 were the dominant SQDG constituents of bathyal and hadal sediments. SQDG-30:0
579 and SQDG-30:2 have been reported in bacteria in North Sea surface waters (Brandsma et al., 2012), in
580 cyanobacteria of the eastern subtropical South Pacific (Van Mooy and Fredricks, 2010), and in plankton detritus

https://doi.org/10.5194/bg-2021-232
Preprint. Discussion started: 3 September 2021

581 from surface sediments of the Black Sea (Schubotz et al., 2009a). Furthermore, SQDG-30:0 is abundant in surface
582 waters of our study area and SQDG-38:4 has been correlated with NO_3^- (Cantarero et al., 2020).
583 The observed differences in the distribution of SQDGs in deep sediments compared to the water column suggests
584 an *in situ* production of previously poorly characterized compounds, and/or lateral transport in addition to at least
585 some export from surface waters.
586
587
588

https://doi.org/10.5194/bg-2021-232
Preprint. Discussion started: 3 September 2021

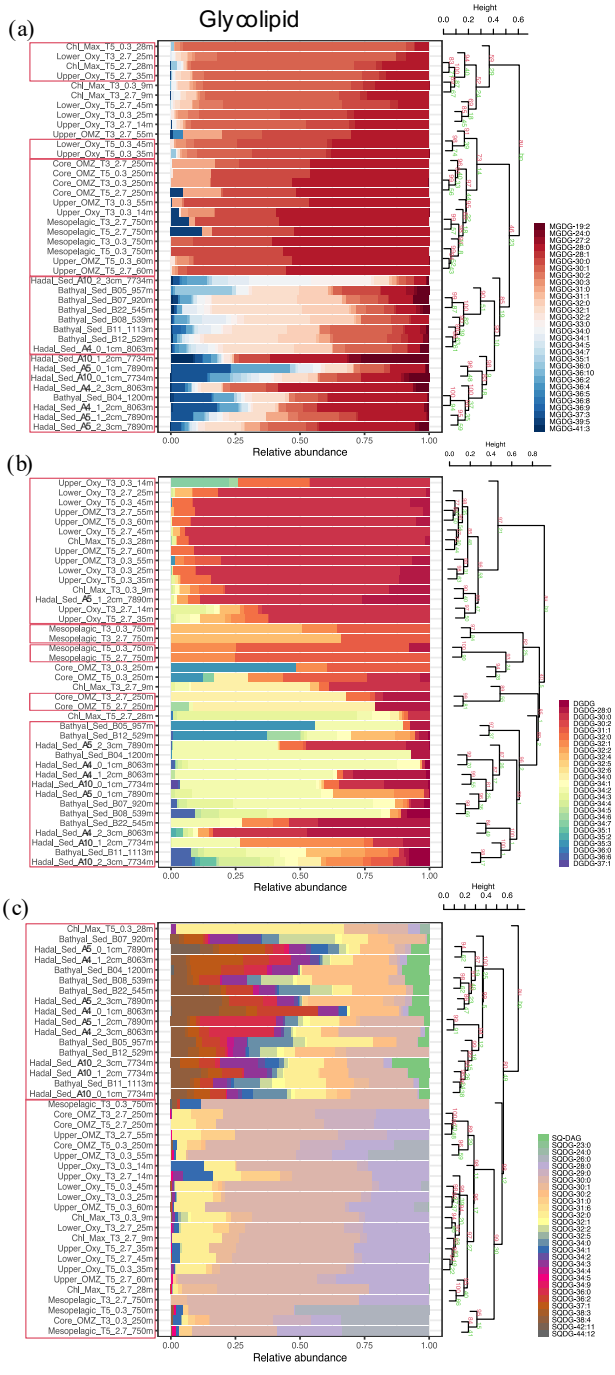

Figure 8. Cumulative bar chart of glycolipid fractional abundances at each sampling station. A) MGDG; B) DGDG; C) SQDG. The number of carbon atoms and unsaturations in core fatty acids follows the order shown in the legend. The right panel depicts a cluster analysis with approximately unbiased (AU) and bootstrap probability (BP) in red and green, respectively, and p-values shown at branching points. The number of bootstrap replicates is 10000. Clusters with AU ≥ 95% confidence are highlighted in red boxes on the left-hand side.

4.4 Potential biological sources of betaine lipids

https://doi.org/10.5194/bg-2021-232
Preprint. Discussion started: 3 September 2021

DGTS (Diacylglyceryl trimethylhomoserine)

DGTSs have diverse biological origins, being found in a wide range of eukaryotes (Sato, 1992; Dembitsky, 1996; Kato et al., 1997; Van Mooy et al., 2009), photoheterotrophic bacteria (Benning et al., 1995; Geiger et al., 1999), photoautotrophic bacteria (Popendorf et al., 2011b) including cyanobacteria (Řezanka et al., 2003), and members of the α-Proteobacteria subdivision (López-Lara et al., 2003). Schubotz et al. (2018) showed DGTS with varying fatty-acid compositions in the OMZ system of the eastern tropical North Pacific, especially in OMZ waters, indicating that these compounds can be biosynthesized by a wider range of source organisms than previously thought.

Consistent with other IPL classes, DGTSs of the bathyal and hadal samples were grouped in the same cluster (AU p-value of 98%) and differed from the water column (Fig. 9a). However, several DGTSs are shared between surface waters (9-60 m) and deep sediments. Indeed, the most abundant DGTSs in bathyal and hadal sediments (DGTS-34:0, DGTS-32:1, DGTS-26:0, DGTS-34:1, DGTS-32:0, and DGTS-25:0; Fig. 9a) are also prominent in the chlorophyll maximum in the eastern subtropical South Pacific (Van Mooy and Fredricks, 2010, and Cantarero et al., 2020). Therefore, their presence in hadal sediments suggest the export of labile organic matter from the euphotic zone, although we cannot rule out other sources.

DGTA (Diacylglyceryl hydroxymethyl-trimethyl-β-alanine)

DGTAs have been widely reported in eukaryotic phytoplankton (Araki et al., 1991; Dembitsky, 1996; Cañavate et al., 2017), mainly in diatoms (Volkman et al., 1989; Zhukova, 2005; Gómez-Consarnau et al., 2007), and are also especially abundant in cultures of Prymnesiophytes and Cryptophytes (Kato et al., 1997). DGTAs have also been found in cyanobacteria (Brandsma et al., 2012) and heterotrophic bacteria (Popendorf et al., 2011a; Sebastián et al., 2016).

DGTAs in bathyal and hadal sediments are mainly composed of longer (C_{28}-C_{42}) and polyunsaturated (1-12) fatty acids compared to those present in the shallowest region of the overlying water column, composed of shorter and saturated fatty acids (Fig. 9b). In the overlying water column, these compounds are associated with relatively high chlorophyll and O_2 concentrations (Cantarero et al., 2020), similar to North Sea surface waters (Brandsma et al., 2012). To the best of our knowledge, the dominant DGTAs in hadal and bathyal sediments (Fig. 9b) have not been previously reported as dominant IPLs in other environments. Whereas no specific biological sources in hadal sediments are known, the structures containing between 30 and 38 carbon atoms might be characteristic of this type of environment.

DGCC (Diacylglycerylcarboxy-N-hydroxymethyl-choline)

Our knowledge of DGCC sources is limited. They have been found in membranes of Prymnesiophyte algae (Kato et al., 1994), mainly in *Pavlova lutheria* (Kato et al., 1994; Eichenberger and Gribi, 1997), and in *E. huxleyi* (Volkman et al., 1989; Pond and Harris, 1996; Van Mooy and Fredricks, 2010). Additionally, they have also been reported in the diatom *Thalassiosira pseudonana* (Van Mooy et al., 2009).

The most abundant IPL from the entire data set of Bathyal and hadal sediments is DGCC-42:6 (Fig. 9c). This is the compound with more C atoms in all IPLs in this study, and with 6 unsaturations. DGCCs with long-chain, polyunsaturated fatty acids (i.e., $C_{38:6}$, $C_{40:10}$, $C_{42:11}$, $C_{44:12}$) have been previously reported in phytoplankton

https://doi.org/10.5194/bg-2021-232
Preprint. Discussion started: 3 September 2021

(Hunter, 2015; Van Mooy and Fredricks, 2010). However, the most abundant DGCCs in hadal sediments have, to the best of our knowledge, not been previously reported, which highlights their potential as biomarkers of deep-sea sediments. However, 3 hadal stations clustered in a separate group (see Fig. 9c), were dominated by DGCC-27:0, and did not contain DGCC-42:6, indicating that this IPL probably comes from lateral transport of organic matter in the rest of the hadal samples.

4.5 Potential biological sources of other lipids

Glycosidic ceramides (Gly-Cer) have been reported in eukaryotic algae such as Prymnesiophyte (Vardi et al., 2009), and have also been shown to be abundant in water columns of OMZ systems (Schubotz et al., 2009b, 2018; Cantarero et al., 2020). In general, the overlying water column shows Gly-Cer with polyunsaturated fatty acids with $C_{21\text{-}38}$. However, these structures are scarce in the bathyal and hadal sediments (see Fig. S6b), which could reflect a deficient export from surface waters due to intense remineralization. On the other hand, Ornithine lipids (OL), phosphatidylinositol (PI), PC-AEGs and other unidentified phospholipids were also present in deep sediments (Fig. S6b). Some PIs and OLs have been reported in sulfate-reducing bacteria (Sturt et al., 2004; Bühring et al., 2014), whereas PC-AEGs have been reported in bacteria inhabiting water columns with reduced oxygen concentration (Schubotz et al., 2018b). Thus, the high relative abundance of PI-AR and PC-AEG-34:3 in hadal and bathyal sediments (Figs. S6b and S7) could be indicative of anaerobic microbial processes. In particular, PI-AR have been related to archaea (Morii et al., 2014), suggesting a high abundance of these microbes in hadal and bathyal sediments. Members of the archaeal domain have already been reported to be abundant in hadal sediments (Xu et al., 2020), however, GDGTs are better markers to explore the IPL content of their membranes (Liu et al., 2011) than those we use here, which warrants further investigation.

Although we cannot confidentially rule out other sources, it is likely that these IPLs in the AT sediments are derived from *in situ* microbial processes, and/or from the transport of labile organic matter from shallower sediment. In particular PI-AR and PC-AEG-34:3 contributed the most to the dissimilarity between the cluster containing only hadal sediment samples (Cluster 1 in Figs. 2, and 3), thus suggesting an *in situ* microbial production. While IPLs can derive from multiple biological sources, we lack data on the largely uncharacterized hadal endemic microbial community, and existing IPL data from the water column does not take into account temporal variability of their biological sources, our study represents a step forward on the characterization of labile sources of organic matter sustaining hadal ecosystems.

https://doi.org/10.5194/bg-2021-232
Preprint. Discussion started: 3 September 2021

Biogeosciences
Discussions
Open Access
EGU

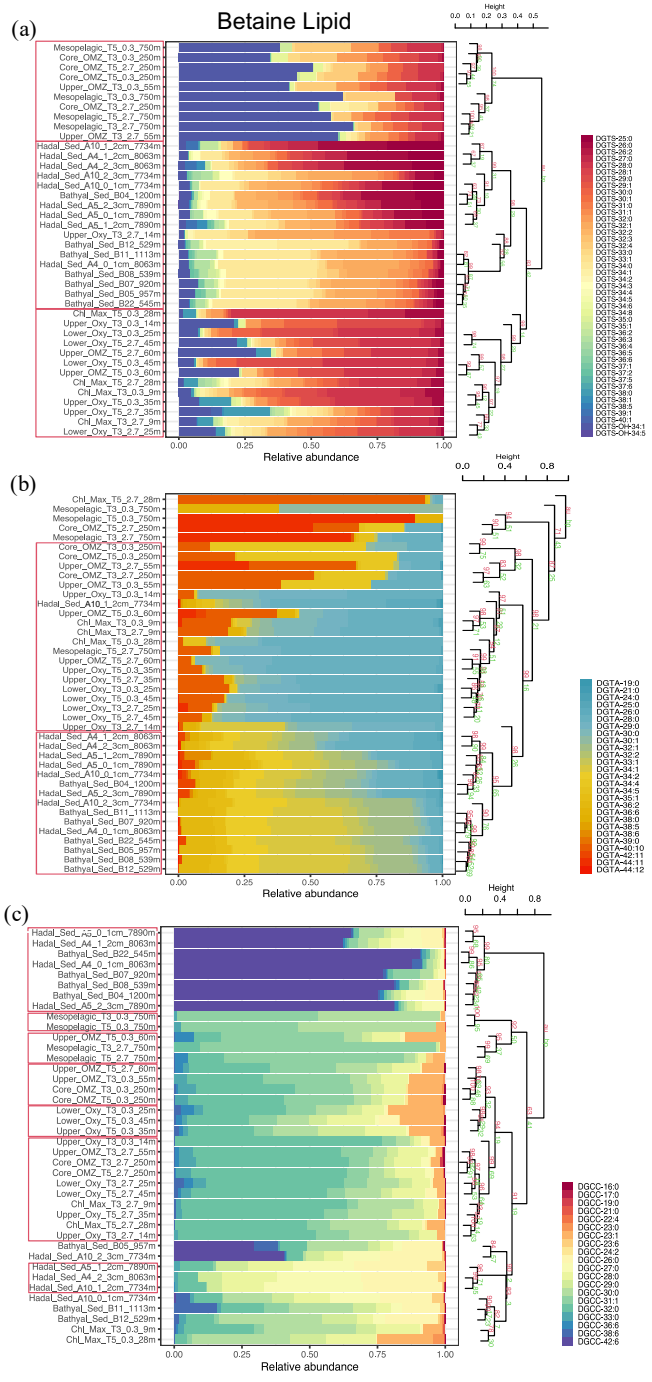

Figure 9. Cumulative bar chart of betaine fractional abundances at each sampling station. A) DGTS; B) DGTA; C) DGCC. The number of carbon atoms and unsaturations core fatty acids follow the order shown in the legend. The right panel depicts a cluster analysis with approximately unbiased (AU) and bootstrap probability (BP) in red and green, respectively, and p-values shown at branching points. The number of bootstrap replicates is 10000. Clusters with AU ≥ 95% confidence are highlighted in red boxes on the left-hand side.

https://doi.org/10.5194/bg-2021-232
Preprint. Discussion started: 3 September 2021

4.6 Allochthonous versus autochthonous IPLs in the Atacama Trench

Given their rapid degradation after cell death (White et al., 1979; Harvey et al., 1986), IPLs are typically considered markers of living or recently dead cells (White et al., 1979; Harvey et al., 1986; Petersen et al., 1991; Lipp et al., 2008). The distribution of IPLs in bathyal and hadal sediments exhibits a high degree of similitude, as demonstrated by the hierarchical analysis (Cluster 1 in Fig. 10a), the NMDS (Fig. 10b), and the SIMPER analysis (Cluster 1 in Table S1). The deep-sea surface sediments showed weak clustering with the IPLs reported in the overlying water column by Cantarero et al. (2020) (Fig 9a). Additionally, water column samples exhibit a larger degree of separation than sediments (ANOSIM, R = 0.78; P <0.01; Fig. 10b) and are broadly clustered by geochemical environments (Cantarero et al., 2020). The low abundance of IPLs characteristic of organisms inhabiting the chlorophyll maximum in deep-sea sediments of the AT (<0.005 % of the total IPL pool; Fig. S3) suggests minimal export of labile organic compounds from the upper ocean, likely due to intense degradation through transit in the water column. Indeed, by using the experimentally calculated kinetic degradation rate constants (k') of ester-bound IPLs by Logemann et al. (2011), and the sinking rate of particles from surface waters to 4000 m (20-100 m/day; Billett et al., 1983; Danovaro et al., 2014), we calculated that ~86-98% ($k'_{t=80}$= 0.033 and $k'_{t=400}$= 0.011) of IPLs from surface waters should degrade by the time that particles reach depths of ~8000 m. These results are in accord with studies indicating elevated benthic oxygen consumption rates resulting from intense microbial respiration of sinking organic matter reaching the sediment (Glud et al., 2013; Wenzhöfer et al., 2016). Thus, the pool of IPLs in hadal sediments appears to predominantly represents *in situ* microbial production and/or lateral sediment transport from shallower depths, and is likely that the deep-sea microbial communities in both benthic and hadal sediments is similar despite their bathymetric zonation (~1,000-8,000 m). Alternatively, we cannot rule out the possibility of new IPL production, particularly from heterotrophic and chemoautotrophic bacteria in micro niches of sinking particles, reaching the deep-sea.

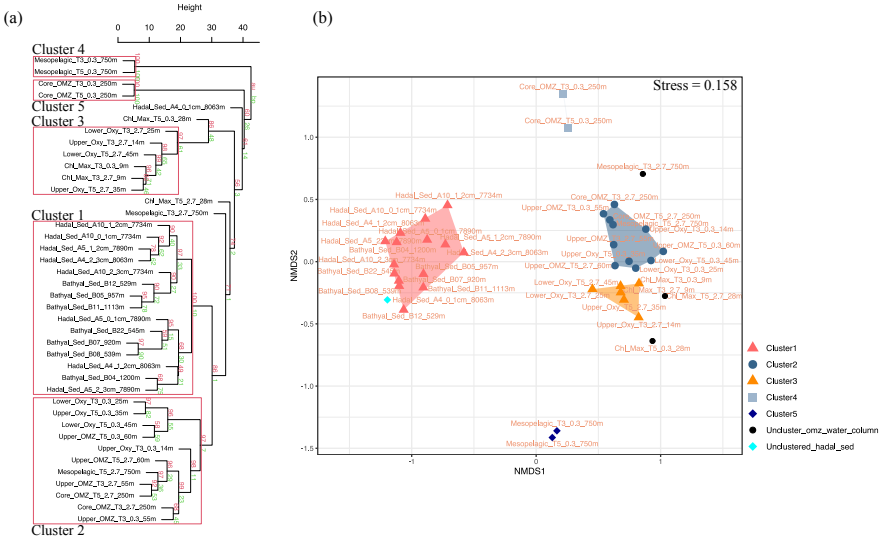

Figure 10. (a) Arithmetic mean (UPGMA) hierarchical clustering based on Euclidean distances calculated from IPLs in each sampling station. Red values are Approximately Unbiased (AU) p-values and green values are Bootstrap Probability (BP) for

https://doi.org/10.5194/bg-2021-232
Preprint. Discussion started: 3 September 2021

each node. Red boxes highlight clusters with 95% confidence. The number of bootstrap replicates is 10000. (b) Non-metric multidimensional scaling (NMDS) analysis of IPLs at each sampling station. The distance matrix was calculated based on the Bray–Curtis dissimilarity. The stress value of the final configuration was 15.8 %. Different symbols and colors represent the sample grouping from hierarchical clusters shown in panel a.

Marine trenches receive organic carbon from a variety of sources and transport mechanisms. These include canyons and river systems that channel organic matter from land to coastal regions, aeolian transport, surface water productivity, and *in situ* production, to name a few (Wenzhöfer et al., 2016; Tarn et al., 2016; Luo et al., 2017; Xu et al., 2018; Guan et al., 2019; Xu et al., 2021). Carbon flux events can increase the delivery of particulate carbon from surface waters to the seafloor (Poff et al., 2021), whereas river discharge and aeolian transport can result in enhanced terrestrial carbon (Xu et al., 2021). Mass wasting events are also known to create dynamic depositional conditions and strong spatial heterogeneity in organic matter distribution in marine trenches (Schauberger et al., 2021; Xu et al., 2021). While marine organic carbon appears to dominate sediments from the Japan (Schwestermann et al., 2021) Massau, and New Britain (Xu et al., 2020) trenches, Xu et al. (2021), using elemental ratios of organic matter, proposed that the Atacama and Kermadec Trenches contain a larger contribution of terrigenous organic matter. Given the labile nature of ester-bond eukaryotic and bacterial IPLs (Lipp et al., 2008; Schouten et al., 2010; Logemann et al., 2011), our study indicates that indigenous organic matter from *in situ* microbial production dominates the pool of labile organic carbon in sediments of the AT and the bathyal region. However, since IPLs do not allow us to estimate the contribution of refractory organic matter coming from allochthonous sources, further work on IPL degradation products and other lipid classes is warranted.

4.7. Characteristic IPLs of hadal and bathyal sediments

The IPLs that contribute most to the dissimilarity between the hierarchical cluster containing samples from the hadal and bathyal sediments (Cluster 1 of Fig. 10) and the water column (cluster 2, 3, 4 and 5 of Fig. 10) are represented in Fig. 11. The most characteristic IPLs of hadal and bathyal sediments are: DGCC-42:6, DGCC-27:0, DGCC-26:0, PC-35:0, PC-30:1, PC-30:2, PC-33:2, PC-32:1, PC-29:2, PE-DAG-32:1, PE-DAG-32:2, PE-DAG-33:1, PI-AR, PG-DAG-36:2, and DGDG-34:2, which we propose as potential markers for these environments. Even though DGCCs have been mainly related to algae membranes (Kato et al., 1994; Van Mooy et al., 2009), DGCCs were minor components of the water column in this area, suggesting a different source for these IPLs. In addition to DGCC, the other two betaine lipids, DGTA and DGTS, exhibited five IPLs that were almost exclusively present in sediment samples (DGTA-34:1, DGTA-32:1, DGTA-34:2, DGTS-34:0 and DGTS-32:1, see Figure 11). We note that almost all the PC phospholipids in our study have not, to the best of our knowledge, been previously reported in the literature, which reinforces their use as markers of *in situ* bathyal and hadal production in sediments.

https://doi.org/10.5194/bg-2021-232
Preprint. Discussion started: 3 September 2021

741 The presence of a few MGDGs and SQs in hadal and bathyal sediments indicates that at least some labile organic
742 matter could derive from the shallow water column (see section 4.3). However, the most abundant IPLs in our
743 sediment samples, DGCC-42:6, PC-35:0, PI-AR, PE-DAG-32:1 and PG-DAG-36:2 (Fig. S7), are almost
744 completely absent in the overlying water column (Fig. 11). This reinforces the idea that these IPLs most likely
745 originate from *in situ* microbial production in sediments.
746
747 The most abundant IPL in sediments, DGCC-42:6, was not present in cluster 1, which only contains hadal
748 sediments (Figs. 2 and 3). Instead, this compound is prominent in clusters 3, 4, and 5, which contain both hadal
749 and bathyal samples. Thus, this IPL appears to be an indicator of lateral transport from bathyal regions, as could
750 be PC-35:0, which has the lowest relative abundance in the cluster only containing hadal sediments. The other
751 highly abundant IPLs in sediment and the hadal cluster (cluster 1 in Fig. 3), PI-AR, PE-DAG-32:1 and PG-DAG-
752 36:2, are also likely indicators of *in situ* microbial biomass. Finally, we acknowledge that temporal variability in
753 IPL production in the upper water column could complicate some of these assignments. For example, while PG-
754 DAG-36:2 was not present in the overlying water column of the Atacama Trench (Fig. 11), it has been previously
755 related to heterotrophic bacteria in surface waters of the South Pacific Ocean (Van Mooy and Fredricks, 2010).
756 Thus, future studies on the temporal variability of IPLs produced in the water column (and sediments) would
757 strengthen some of the associations we see in our data.
758
759

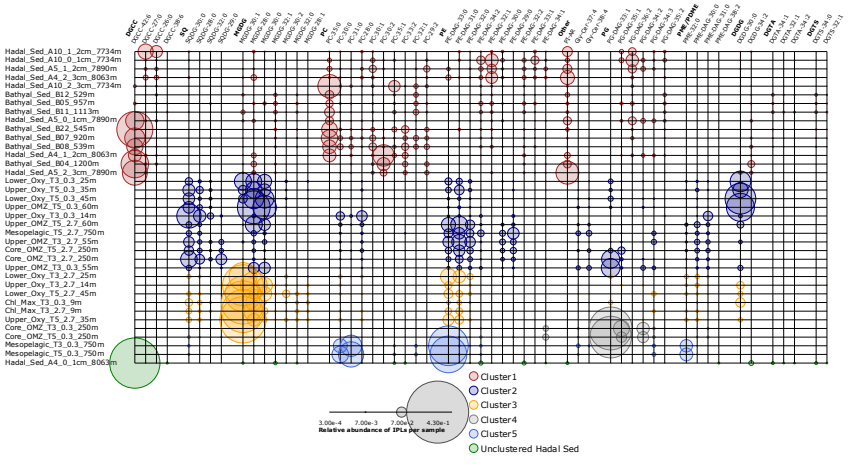

760
761
762 **Figure 11. Relative abundance of individual IPLs that contribute most to the dissimilarity between clusters of Fig. 10**
763 **derived from the SIMPER analysis (Table S1). Circle ratios are proportional to the relative abundance of IPL**
764 **compounds per sample. Samples are organized along the Y axis and shown in colors that match the hierarchical cluster**
765 **analysis in Fig. 10. The scale for circumference size is shown in the legend.**
766
767

768
769

https://doi.org/10.5194/bg-2021-232
Preprint. Discussion started: 3 September 2021

770 **4.8 Do IPLs reveal homeoviscous adaptation to the deep-sea environment?**
771
772 Environmental factors such as pH, conductivity, temperature, and pressure impact the permeability and fluidity
773 of cell membranes (Shaw, 1974; Macdonald, 1984; DeLong and Yayanos, 1985; Somero, 1992; Komatsu and
774 Chong, 1998; Van Mooy et al., 2009; Carini et al., 2015; Sebastián et al., 2016; Siliakus et al., 2017; Boyer et al.,
775 2020). Thus, organisms adapt to changes in environmental factors to maintain physiological homeostasis by
776 altering their fatty acid composition (DeLong and Yayanos, 1985; Fang et al., 2000; Nichols et al., 2004; Siliakus
777 et al., 2017). The combined physiological effects of high hydrostatic pressure and low temperature on prokaryotic
778 membranes in laboratory cultures leads to the production of unsaturated lipids (DeLong and Yayanos 1985; Fang
779 et al., 2000; Nichols et al., 2004; Zheng et al., 2020). However, few studies have been conducted using culture-
780 independent techniques in search for potential adaptation mechanisms in organisms inhabiting the deep ocean
781 (i.e., Zhong et al., 2020). We sought to understand whether the chemical composition of core fatty acids within
782 different IPL classes (i.e., carbon length and unsaturation degree) reflects the combined effects of the low
783 temperature and high pressure typical of hadal settings. We show that PGs are abundant in hadal sediments of the
784 AT (Fig. S4). Fang et al., (2000) using strains isolated from Mariana Trench sediments, found that PG was the
785 most abundant class of phospholipids and presumed that it could be a physiological response to high pressure and
786 low temperature, subsequent studies have confirmed this approach (Winter et al., 2009; Periasamy et al., 2009;
787 Jebbar et al., 2015, Allemann et al., 2021). Cluster 1 in the boxplot analysis (Fig. 4) likely contains the most
788 characteristic IPL classes of the hadal zone. In general, the phospholipid class in this cluster exhibited
789 comparatively fatty acid chains that are monounsaturated and saturated compared to other environments (Figs.
790 4a, b). Additionally, we observed an increase in the ratio of total unsaturated to saturated fatty acids in deep
791 sediments compared to the water column (Fig. 5), which could reflect physiological adaptations of their biological
792 producers. These results are in accord with studies indicating biosynthesis and incorporation of polyunsaturated
793 fatty acids into phospholipid membranes of piezophilic bacteria (DeLong and Yayanos, 1985; Baird et al., 1985;
794 Yano et al., 1998; Winter, 2002; Mangelsdorf et al., 2005; Winter and Jeworrek, 2009; Allemann et al., 2021).
795 Thus, the chemical characteristics (C length and degree of unsaturation) of the most abundant IPLs in sediments
796 of the AT suggest homeoviscous adaptation to this type of environment by their source organisms, in addition to
797 potentially indicating the occurrence of compounds that are unique to the endogenous community.
798
799 **5. Conclusions**
800
801 IPLs in surface hadal sediments from the deepest points of the Atacama Trench share characteristics with those
802 in bathyal sediments and differ from those found in particles from the upper ocean, including the euphotic zone
803 and the oxygen minimum zone. This suggests that IPLs in the hadal region are most representative of lateral
804 sediment transport from shallower depths combined with *in situ* microbial production.
805
806 The most dominant IPL structures in the bathyal and hadal sediments show a great variety of phospholipids with
807 varying degrees of unsaturation that are likely bacterial in origin. Hadal sediments also exhibit unique glycolipid
808 structures such as SQDG-42:11, SQDG-23:0, DGDG-35:1, DGDG-35:2 and DGDG-37:1 that have not, to the
809 best of our knowledge, been reported in other environments. Although, they are present in low abundance and
810 represent a small fraction (~0.00012%) of the total IPL pool in sediments. Furthermore, hadal sediments exhibited
811 high spatial heterogeneity in IPL distribution. The similarities in IPLs between hadal and bathyal sediments

https://doi.org/10.5194/bg-2021-232
Preprint. Discussion started: 3 September 2021

supports lateral transport of organic matter or the occurrence of potentially similar *in situ* bacterial communities with traits such as mono-unsaturated and high ratios of unsaturated/saturated fatty acids that possibly indicate homeoviscous adaptation to the high pressure and low temperatures found in deep-sea environments.

An improved understanding of the phylogenetic and metabolic association of IPLs, as well as their ecological role in this unique and extreme environment, could be achieved in future studies by including a detailed analysis of the biogeochemical conditions as well as the composition of the microbial community in hadal sediments from the Atacama trench.

Author contribution

EF, OU, and JS designed the study. MZ contributed with the hadal samples from the HADES-ERC cruise. EF prepared, extracted, and analyzed samples from the HADES-ERC cruise with help from SC and ND under the supervision of JS. EF and SC processed results. EF, SC, and JS interpreted results. EF and PR-F performed statistical analyses. EF wrote the manuscript with contributions from SC, JS, and OU. All authors provided feedback on the manuscript. OU and JS funded the research.

Competing interests

The authors declare that they have no conflict of interest.

Acknowledgements

This work was supported by the Chilean Agency for Research and Development (grants ICN12_019-IMO and FONDECYT 1191360 to O. Ulloa). Additional support was provided by the Department of Geological Sciences and INSTAAR at the University of Colorado Boulder (to J. Sepúlveda), the European Research Council (Hades-ERC, grant agreement number 669947, to R.N. Glud), and the Max Planck Society. EF was also partially supported by the UCO 1866 Student Scholarship-2019, Directorate of Graduate Studies, Universidad of Concepción. We are thankful to the captains, crews, and scientists of the German RV *Sonne* cruises SO-261 (HADES-ERC) and SO-211 (ChiMeBo). In particular, we thank the chief scientists R.N. Glud and F. Wenzhöfer (HADES-ERC) and D. Hebbeln (ChiMeBo). The HADES-ERC and ChiMeBo cruises were funded by the European Research Council and the German Bundesministerium für Bildung & Forschung (BMBF), respectively. We also wish to thank Carina Lange and Silvio Pantoja for access to samples from the ChiMeBo cruise and M. Pizarro-Koch for the preparation of the three-dimensional map. We also wish to thank L. Nuñez, B. Srain, R. Castro, A. Ávila, M. Mohtadi, R. De Pol-Holz, and G. Martínez-Méndez, for sample collection during the ChiMeBo cruise and/or laboratory assistance.

https://doi.org/10.5194/bg-2021-232
Preprint. Discussion started: 3 September 2021

References

Ahumada, R.: Producción y destino de la biomasa fitoplanctónica en un sistema de bahías en Chile central: una hipótesis, Biol PesqChile, 18, 53–66, 1989.

Allemann, M. N. and Allen, E. E.: Genetic suppression of lethal mutations in fatty acid biosynthesis mediated by a secondary lipid synthase, Appl. Environ. Microbiol., 87, 2021.

Allen, E. E., Facciotti, D., and Bartlett, D. H.: Monounsaturated but not polyunsaturated fatty acids are required for growth of the deep-sea bacteriumPhotobacterium profundum SS9 at high pressure and low temperature, Appl. Environ. Microbiol., 65, 1710–1720, 1999.

Angel, M.: Detrital organic fluxes through pelagic ecosystems, in: Flows of energy and materials in marine ecosystems, Springer, 475–516, 1984.

Angel, M. V.: Ocean trench conservation, Environmentalist, 2, 1–17, 1982.

Araki, S., Eichenberger, W., Sakurai, T., and Sato, N.: Distribution of diacylglycerylhydroxymethyltrimethyl-β-alanine (DGTA) and phosphatidylcholine in brown algae, Plant Cell Physiol., 32, 623–628, 1991.

Baird, B.: Biomass and community structure of the abyssal microbiota determined from basin and Puerto Rico trench sediments, Benthic Ecol. Sediment. Process. Venezuela Basin-Past Present, 61, 217–213, 1985.

Bao, R., Strasser, M., McNichol, A. P., Haghipour, N., McIntyre, C., Wefer, G., and Eglinton, T. I.: Tectonically-triggered sediment and carbon export to the Hadal zone, Nat. Commun., 9, 1–8, 2018.

Barridge, J. K. and Shively, J.: Phospholipids of the Thiobacilli, J. Bacteriol., 95, 2182–2185, 1968.

Batrakov, S. G. and Nikitin, D. I.: Lipid composition of the phosphatidylcholine-producing bacterium Hyphomicrobium vulgare NP-160, Biochim. Biophys. Acta BBA-Lipids Lipid Metab., 1302, 129–137, 1996.

Benning, C., Huang, Z.-H., and Gage, D. A.: Accumulation of a novel glycolipid and a betaine lipid in cells of Rhodobacter sphaeroides grown under phosphate limitation, Arch. Biochem. Biophys., 317, 103–111, 1995.

Bergé, J.-P. and Barnathan, G.: Fatty acids from lipids of marine organisms: molecular biodiversity, roles as biomarkers, biologically active compounds, and economical aspects, Mar. Biotechnol. I, 49–125, 2005.

Biddle, J. F., Lipp, J. S., Lever, M. A., Lloyd, K. G., Sørensen, K. B., Anderson, R., Fredricks, H. F., Elvert, M., Kelly, T. J., Schrag, D. P., and others: Heterotrophic Archaea dominate sedimentary subsurface ecosystems off Peru, Proc. Natl. Acad. Sci., 103, 3846–3851, 2006.

Billett, D., Lampitt, R., Rice, A., and Mantoura, R.: Seasonal sedimentation of phytoplankton to the deep-sea benthos, Nature, 302, 520–522, 1983.

Bligh, E. G. and Dyer, W. J.: A rapid method of total lipid extraction and purification, Can. J. Biochem. Physiol., 37, 911–917, 1959.

https://doi.org/10.5194/bg-2021-232
Preprint. Discussion started: 3 September 2021

883 Boyer, G. M., Schubotz, F., Summons, R. E., Woods, J., and Shock, E. L.: Carbon oxidation state in microbial
884 polar lipids suggests adaptation to hot spring temperature and redox gradients, Front. Microbiol., 11, 229, 2020.

885 Brandsma, J., Hopmans, E., Philippart, C., Veldhuis, M., Schouten, S., and Damsté, J. S.: Temporal variations in
886 abundance and composition of intact polar lipids in North Sea coastal marine water, Biogeosciences Discuss., 8,
887 8895, 2011.

888 Brandsma, J., Hopmans, E., Philippart, C., Veldhuis, M., Schouten, S., and Sinninghe Damsté, J.: Low temporal
889 variation in the intact polar lipid composition of North Sea coastal marine water reveals limited chemotaxonomic
890 value, Biogeosciences, 9, 1073–1084, 2012.

891 Bühring, S. I., Kamp, A., Wörmer, L., Ho, S., and Hinrichs, K.-U.: Functional structure of laminated microbial
892 sediments from a supratidal sandy beach of the German Wadden Sea (St. Peter-Ording), J. Sea Res., 85, 463–473,
893 2014.

894 Cañavate, J. P., Armada, I., and Hachero-Cruzado, I.: Interspecific variability in phosphorus-induced lipid
895 remodelling among marine eukaryotic phytoplankton, New Phytol., 213, 700–713, 2017.

896 Cantarero, S. I., Henríquez-Castillo, C., Dildar, N., Vargas, C. A., Von Dassow, P., Cornejo-D'Ottone, M., and
897 Sepúlveda, J.: Size-fractionated contribution of microbial biomass to suspended organic matter in the eastern
898 Tropical South Pacific oxygen minimum zone, Front. Mar. Sci., 7, 745, 2020.

899 Carini, P., Van Mooy, B. A., Thrash, J. C., White, A., Zhao, Y., Campbell, E. O., Fredricks, H. F., and Giovannoni,
900 S. J.: SAR11 lipid renovation in response to phosphate starvation, Proc. Natl. Acad. Sci., 112, 7767–7772, 2015.

901 Clarke, K. and Gorley, R.: Getting started with PRIMER v7, Primer-E Plymouth Plymouth Mar. Lab., 20, 2015.

902 da Costa, E., Amaro, H. M., Melo, T., Guedes, A. C., and Domingues, M. R.: Screening for polar lipids,
903 antioxidant, and anti-inflammatory activities of Gloeothece sp. lipid extracts pursuing new phytochemicals from
904 cyanobacteria, J. Appl. Phycol., 32, 3015–3030, 2020.

905 Danovaro, R., Della Croce, N., Dell'Anno, A., and Pusceddu, A.: A depocenter of organic matter at 7800 m depth
906 in the SE Pacific Ocean, Deep Sea Res. Part Oceanogr. Res. Pap., 50, 1411–1420, 2003.

907 Danovaro, R., Snelgrove, P. V., and Tyler, P.: Challenging the paradigms of deep-sea ecology, Trends Ecol. Evol.,
908 29, 465–475, 2014.

909 DeLong, E. F. and Yayanos, A. A.: Adaptation of the membrane lipids of a deep-sea bacterium to changes in
910 hydrostatic pressure, Science, 228, 1101–1103, 1985.

911 Dembitsky, V. M.: Betaine ether-linked glycerolipids: chemistry and biology, Prog. Lipid Res., 35, 1–51, 1996.

912 Dowhan, W.: Molecular basis for membrane phospholipid diversity: why are there so many lipids?, Annu. Rev.
913 Biochem., 66, 199–232, 1997.

https://doi.org/10.5194/bg-2021-232
Preprint. Discussion started: 3 September 2021

914 Eichenberger, W. and Gribi, C.: Lipids of Pavlova lutheri: cellular site and metabolic role of DGCC,
915 Phytochemistry, 45, 1561–1567, 1997.

916 Eloe, E. A., Shulse, C. N., Fadrosh, D. W., Williamson, S. J., Allen, E. E., and Bartlett, D. H.: Compositional
917 differences in particle-associated and free-living microbial assemblages from an extreme deep-ocean
918 environment, Environ. Microbiol. Rep., 3, 449–458, 2011.

919 Fang, J., Barcelona, M. J., Nogi, Y., and Kato, C.: Biochemical implications and geochemical significance of
920 novel phospholipids of the extremely barophilic bacteria from the Marianas Trench at 11,000 m, Deep Sea Res.
921 Part Oceanogr. Res. Pap., 47, 1173–1182, 2000.

922 Fernández-Urruzola, I., Ulloa, O., Glud, R., Pinkerton, M., Schneider W., Wenzhöfer, F. and Escribano, R:
923 Plankton respiration in the Atacama Trench region: Implications for particulate organic carbon fux into the hadal
924 realm, Limnol. Oceanogr., 2021.

925 Fischer, J. P., Ferdelman, T. G., D'Hondt, S., Røy, H., and Wenzhöfer, F.: Oxygen penetration deep into the
926 sediment of the South Pacific gyre, Biogeosciences, 6, 1467–1478, 2009.

927 Gašparović, B., Penezić, A., Frka, S., Kazazić, S., Lampitt, R. S., Holguin, F. O., Sudasinghe, N., and Schaub, T.:
928 Particulate sulfur-containing lipids: Production and cycling from the epipelagic to the abyssopelagic zone, Deep
929 Sea Res. Part Oceanogr. Res. Pap., 134, 12–22, 2018.

930 Geiger, O., Röhrs, V., Weissenmayer, B., Finan, T. M., and Thomas-Oates, J. E.: The regulator gene phoB
931 mediates phosphate stress-controlled synthesis of the membrane lipid diacylglyceryl-N, N, N-
932 trimethylhomoserine in Rhizobium (Sinorhizobium) meliloti, Mol. Microbiol., 32, 63–73, 1999.

933 Glud, R. N., Wenzhöfer, F., Middelboe, M., Oguri, K., Turnewitsch, R., Canfield, D. E., and Kitazato, H.: High
934 rates of microbial carbon turnover in sediments in the deepest oceanic trench on Earth, Nat. Geosci., 6, 284–288,
935 2013.

936 Glud, R. N., Berg, P., Thamdrup, B., Larsen, M., Stewart, H. A., Jamieson, A. J., Glud, A., Oguri, K., Sanei, H.,
937 Rowden, A. A., and others: Hadal trenches are dynamic hotspots for early diagenesis in the deep sea, Commun.
938 Earth Environ., 2, 1–8, 2021.

939 Goldfine, H.: Bacterial membranes and lipid packing theory, J. Lipid Res., 25, 1501–1507, 1984.

940 Goldfine, H. and Hagen, P.-O.: N-Methyl groups in bacterial lipids III. phospholipids of hyphomicrobia, J.
941 Bacteriol., 95, 367–375, 1968.

942 Gombos, Z., Várkonyi, Z., Hagio, M., Iwaki, M., Kovács, L., Masamoto, K., Itoh, S., and Wada, H.:
943 Phosphatidylglycerol requirement for the function of electron acceptor plastoquinone QB in the photosystem II
944 reaction center, Biochemistry, 41, 3796–3802, 2002.

https://doi.org/10.5194/bg-2021-232
Preprint. Discussion started: 3 September 2021

945 Gómez-Consarnau, L., González, J. M., Coll-Lladó, M., Gourdon, P., Pascher, T., Neutze, R., Pedrós-Alió, C.,
946 and Pinhassi, J.: Light stimulates growth of proteorhodopsin-containing marine Flavobacteria, Nature, 445, 210–
947 213, 2007.

948 Gooday, A. J., Bett, B. J., Escobar, E., Ingole, B., Levin, L. A., Neira, C., Raman, A. V., and Sellanes, J.: Habitat
949 heterogeneity and its influence on benthic biodiversity in oxygen minimum zones, Mar. Ecol., 31, 125–147, 2010.

950 Gounaris, K. and Barber, J.: Monogalactosyldiacylglycerol: the most abundant polar lipid in nature, Trends
951 Biochem. Sci., 8, 378–381, 1983.

952 Guan, H., Chen, L., Luo, M., Liu, L., Mao, S., Ge, H., Zhang, M., Fang, J., and Chen, D.: Composition and origin
953 of lipid biomarkers in the surface sediments from the southern Challenger Deep, Mariana Trench, Geosci. Front.,
954 10, 351–360, 2019.

955 Hand, K., Bartlett, D., Fryer, P., Peoples, L., Williford, K., Hofmann, A., and Cameron, J.: Discovery of novel
956 structures at 10.7 km depth in the Mariana Trench may reveal chemolithoautotrophic microbial communities,
957 Deep Sea Res. Part Oceanogr. Res. Pap., 160, 103238, 2020.

958 Harvey, H. R., Fallon, R. D., and Patton, J. S.: The effect of organic matter and oxygen on the degradation of
959 bacterial membrane lipids in marine sediments, Geochim. Cosmochim. Acta, 50, 795–804, 1986.

960 Harwood, J. L.: Membrane lipids in algae, in: Lipids in photosynthesis: structure, function and genetics, Springer,
961 53–64, 1998.

962 Hedges, J. I., Baldock, J. A., Gélinas, Y., Lee, C., Peterson, M., and Wakeham, S. G.: Evidence for non-selective
963 preservation of organic matter in sinking marine particles, Nature, 409, 801–804, 2001.

964 Heinz, E.: Enzymatic reactions in galactolipid biosynthesis, in: Lipids and lipid polymers in higher plants,
965 Springer, 102–120, 1977.

966 Hiraoka, S., Hirai, M., Matsui, Y., Makabe, A., Minegishi, H., Tsuda, M., Rastelli, E., Danovaro, R., Corinaldesi,
967 C., Kitahashi, T., and others: Microbial community and geochemical analyses of trans-trench sediments for
968 understanding the roles of hadal environments, ISME J., 14, 740–756, 2020.

969 Houston, J.: Variability of precipitation in the Atacama Desert: its causes and hydrological impact, Int. J. Climatol.
970 J. R. Meteorol. Soc., 26, 2181–2198, 2006.

971 Hunter, J. E.: Phytoplankton lipidomics: lipid dynamics in response to microalgal stressors, PhD Thesis,
972 University of Southampton, 2015.

973 Ichino, M. C., Clark, M. R., Drazen, J. C., Jamieson, A., Jones, D. O., Martin, A. P., Rowden, A. A., Shank, T.
974 M., Yancey, P. H., and Ruhl, H. A.: The distribution of benthic biomass in hadal trenches: a modelling approach
975 to investigate the effect of vertical and lateral organic matter transport to the seafloor, Deep Sea Res. Part
976 Oceanogr. Res. Pap., 100, 21–33, 2015.

https://doi.org/10.5194/bg-2021-232
Preprint. Discussion started: 3 September 2021

977 Imhoff, J. F.: Taxonomy and physiology of phototrophic purple bacteria and green sulfur bacteria, in: Anoxygenic
978 photosynthetic bacteria, Springer, 1–15, 1995.

979 Inthorn, M., Wagner, T., Scheeder, G., and Zabel, M.: Lateral transport controls distribution, quality, and burial
980 of organic matter along continental slopes in high-productivity areas, Geology, 34, 205–208, 2006.

981 Itoh, M., Kawamura, K., Kitahashi, T., Kojima, S., Katagiri, H., and Shimanaga, M.: Bathymetric patterns of
982 meiofaunal abundance and biomass associated with the Kuril and Ryukyu trenches, western North Pacific Ocean,
983 Deep Sea Res. Part Oceanogr. Res. Pap., 58, 86–97, 2011.

984 Itou, M., Matsumura, I., and Noriki, S.: A large flux of particulate matter in the deep Japan Trench observed just
985 after the 1994 Sanriku-Oki earthquake, Deep Sea Res. Part Oceanogr. Res. Pap., 47, 1987–1998, 2000.

986 Jahnke, R. A. and Jahnke, D. B.: Rates of C, N, P and Si recycling and denitrification at the US Mid-Atlantic
987 continental slope depocenter, Deep Sea Res. Part Oceanogr. Res. Pap., 47, 1405–1428, 2000.

988 Jahnke, R. A., Reimers, C. E., and Craven, D. B.: Intensification of recycling of organic matter at the sea floor
989 near ocean margins, Nature, 348, 50–54, 1990.

990 Jain, S., Caforio, A., and Driessen, A. J.: Biosynthesis of archaeal membrane ether lipids, Front. Microbiol., 5,
991 641, 2014.

992 Jamieson, A. J., Fujii, T., Mayor, D. J., Solan, M., and Priede, I. G.: Hadal trenches: the ecology of the deepest
993 places on Earth, Trends Ecol. Evol., 25, 190–197, 2010.

994 Jebbar, M., Franzetti, B., Girard, E., and Oger, P.: Microbial diversity and adaptation to high hydrostatic pressure
995 in deep-sea hydrothermal vents prokaryotes, Extremophiles, 19, 721–740, 2015.
996
997 Kalisch, B., Dörmann, P., and Hölzl, G.: DGDG and glycolipids in plants and algae, Lipids Plant Algae Dev., 51–
998 83, 2016.

999 Kaneda, T.: Iso-and anteiso-fatty acids in bacteria: biosynthesis, function, and taxonomic significance., Microbiol.
1000 Mol. Biol. Rev., 55, 288–302, 1991.

1001 Kato, C., Masui, N., and Horikoshi, K.: Properties of obligately barophilic bacteria isolated from a sample of
1002 deep-sea sediment from the Izu-Bonin trench, Oceanogr. Lit. Rev., 1, 53–54, 1997.

1003 Kato, M., Adachi, K., Hajiro-Nakanishi, K., Ishigaki, E., Sano, H., and Miyachi, S.: betaine lipid from Pavolova
1004 lutheri, Phytochemistry, 1994.

1005 Kioka, A., Schwestermann, T., Moernaut, J., Ikehara, K., Kanamatsu, T., Eglinton, T. I., and Strasser, M.: Event
1006 stratigraphy in a hadal oceanic trench: The Japan trench as sedimentary archive recording recurrent giant
1007 subduction zone earthquakes and their role in organic carbon export to the deep sea, Front. Earth Sci., 7, 319,
1008 2019.

https://doi.org/10.5194/bg-2021-232
Preprint. Discussion started: 3 September 2021

1009 Koblížek, M., Falkowski, P. G., and Kolber, Z. S.: Diversity and distribution of photosynthetic bacteria in the
1010 Black Sea, Deep Sea Res. Part II Top. Stud. Oceanogr., 53, 1934–1944, 2006.

1011 Koga, Y. and Morii, H.: Biosynthesis of ether-type polar lipids in archaea and evolutionary considerations,
1012 Microbiol. Mol. Biol. Rev., 71, 97–120, 2007.

1013 Komatsu, H. and Chong, P. L.-G.: Low permeability of liposomal membranes composed of bipolar tetraether
1014 lipids from thermoacidophilic archaebacterium Sulfolobus acidocaldarius, Biochemistry, 37, 107–115, 1998.

1015 Lam, P., Jensen, M. M., Lavik, G., McGinnis, D. F., Müller, B., Schubert, C. J., Amann, R., Thamdrup, B., and
1016 Kuypers, M. M.: Linking crenarchaeal and bacterial nitrification to anammox in the Black Sea, Proc. Natl. Acad.
1017 Sci., 104, 7104–7109, 2007.

1018 Lechevalier, H.: Chemotaxonomic use of lipids-an overview, Microb. Lipids, 1, 869–902, 1988.

1019 Leduc, D., Rowden, A. A., Glud, R. N., Wenzhöfer, F., Kitazato, H., and Clark, M. R.: Comparison between
1020 infaunal communities of the deep floor and edge of the Tonga Trench: possible effects of differences in organic
1021 matter supply, Deep Sea Res. Part Oceanogr. Res. Pap., 116, 264–275, 2016.

1022 Lipp, J. S. and Hinrichs, K.-U.: Structural diversity and fate of intact polar lipids in marine sediments, Geochim.
1023 Cosmochim. Acta, 73, 6816–6833, 2009a.

1024 Lipp, J. S. and Hinrichs, K.-U.: Structural diversity and fate of intact polar lipids in marine sediments, Geochim.
1025 Cosmochim. Acta, 73, 6816–6833, 2009b.

1026 Lipp, J. S., Morono, Y., Inagaki, F., and Hinrichs, K.-U.: Significant contribution of Archaea to extant biomass in
1027 marine subsurface sediments, Nature, 454, 991–994, 2008.

1028 Liu, J., Zheng, Y., Lin, H., Wang, X., Li, M., Liu, Y., Yu, M., Zhao, M., Pedentchouk, N., Lea-Smith, D. J., and
1029 others: Proliferation of hydrocarbon-degrading microbes at the bottom of the Mariana Trench, Microbiome, 7, 1–
1030 13, 2019.

1031 Liu, X., Lipp, J. S., and Hinrichs, K.-U.: Distribution of intact and core GDGTs in marine sediments, Org.
1032 Geochem., 42, 368–375, 2011.

1033 Liu, X.-L., Lipp, J. S., Simpson, J. H., Lin, Y.-S., Summons, R. E., and Hinrichs, K.-U.: Mono-and dihydroxyl
1034 glycerol dibiphytanyl glycerol tetraethers in marine sediments: Identification of both core and intact polar lipid
1035 forms, Geochim. Cosmochim. Acta, 89, 102–115, 2012.

1036 Logemann, J., Graue, J., Köster, J., Engelen, B., Rullkötter, J., and Cypionka, H.: A laboratory experiment of
1037 intact polar lipid degradation in sandy sediments, Biogeosciences, 8, 2547–2560, 2011.

1038 López-Lara, I. M., Sohlenkamp, C., and Geiger, O.: Membrane lipids in plant-associated bacteria: their
1039 biosyntheses and possible functions, Mol. Plant. Microbe Interact., 16, 567–579, 2003.

https://doi.org/10.5194/bg-2021-232
Preprint. Discussion started: 3 September 2021

1040 Lund, E. D. and Chu, F.-L. E.: Phospholipid biosynthesis in the oyster protozoan parasite, Perkinsus marinus,
1041 Mol. Biochem. Parasitol., 121, 245–253, 2002.

1042 Luo, M., Gieskes, J., Chen, L., Shi, X., and Chen, D.: Provenances, distribution, and accumulation of organic
1043 matter in the southern Mariana Trench rim and slope: Implication for carbon cycle and burial in hadal trenches,
1044 Mar. Geol., 386, 98–106, 2017.

1045 Macdonald, A.: The effects of pressure on the molecular structure and physiological functions of cell membranes,
1046 Philos. Trans. R. Soc. Lond. B Biol. Sci., 304, 47–68, 1984.

1047 Makula, R.: Phospholipid composition of methane-utilizing bacteria., J. Bacteriol., 134, 771–777, 1978.

1048 Mangelsdorf, K., Zink, K.-G., Birrien, J.-L., and Toffin, L.: A quantitative assessment of pressure dependent
1049 adaptive changes in the membrane lipids of a piezosensitive deep sub-seafloor bacterium, Org. Geochem., 36,
1050 1459–1479, 2005.

1051 Martin, J. H., Knauer, G. A., Karl, D. M., and Broenkow, W. W.: VERTEX: carbon cycling in the northeast
1052 Pacific, Deep Sea Res. Part Oceanogr. Res. Pap., 34, 267–285, 1987.

1053 Matys, E., Sepúlveda, J., Pantoja, S., Lange, C., Caniupán, M., Lamy, F., and Summons, R. E.:
1054 Bacteriohopanepolyols along redox gradients in the Humboldt Current System off northern Chile, Geobiology,
1055 15, 844–857, 2017.

1056 Mayzaud, P., Virtue, P., and Albessard, E.: Seasonal variations in the lipid and fatty acid composition of the
1057 euphausiid Meganyctiphanes norvegica from the Ligurian Sea, Mar. Ecol. Prog. Ser., 186, 199–210, 1999.

1058 Mirzaei, A., Rahmati, M., and Ahmadi, M.: A new method for hierarchical clustering combination, Intell. Data
1059 Anal., 12, 549–571, 2008.

1060 Murata, N. and Siegenthaler, P.-A.: Lipids in photosynthesis: an overview, Lipids Photosynth. Struct. Funct.
1061 Genet., 1–20, 1998.

1062 Morii, H., Ogawa, M., Fukuda, K. and Taniguchi, H. Ubiquitous distribution of phosphatidylinositol phosphate
1063 synthase and archaetidylinositol phosphate synthase in Bacteria and Archaea, which contain inositol phospholipid,
1064 Biochem. Bioph. Res, 275, 36568–36574, 2014.

1065 Nichols, D. S., Miller, M. R., Davies, N. W., Goodchild, A., Raftery, M., and Cavicchioli, R.: Cold adaptation in
1066 the Antarctic archaeon Methanococcoides burtonii involves membrane lipid unsaturation, J. Bacteriol., 186,
1067 8508–8515, 2004.

1068 Nunoura, T., Takaki, Y., Hirai, M., Shimamura, S., Makabe, A., Koide, O., Kikuchi, T., Miyazaki, J., Koba, K.,
1069 Yoshida, N., and others: Hadal biosphere: insight into the microbial ecosystem in the deepest ocean on Earth,
1070 Proc. Natl. Acad. Sci., 112, E1230–E1236, 2015.

https://doi.org/10.5194/bg-2021-232
Preprint. Discussion started: 3 September 2021

1071 Nunoura, T., Hirai, M., Yoshida-Takashima, Y., Nishizawa, M., Kawagucci, S., Yokokawa, T., Miyazaki, J.,
1072 Koide, O., Makita, H., Takaki, Y., and others: Distribution and niche separation of planktonic microbial
1073 communities in the water columns from the surface to the hadal waters of the Japan Trench under the Eutrophic
1074 Ocean, Front. Microbiol., 7, 1261, 2016.

1075 Nunoura, T., Nishizawa, M., Hirai, M., Shimamura, S., Harnvoravongchai P., Koide, O., Morono, Y., Fukui, T.,
1076 Inagaki, F., Miyazaki, J., Takaki, Y., and others: Microbial Diversity in Sediments from the Bottom of the
1077 Challenger Deep, the Mariana Trench, Microbes Environ, 33, 186–194, 2018.

1078 Oksanen, J., Blanchet, F. G., Kindt, R., Legendre, P., Minchin, P., O'hara, R., Simpson, G., Solymos, P., Stevens,
1079 M., Wagner, H., and others: Community ecology package, R Package Version, 2, 2013.

1080 Oliver, J. D. and Colwell, R. R.: Extractable lipids of gram-negative marine bacteria: phospholipid composition,
1081 J. Bacteriol., 114, 897–908, 1973.

1082 Patton, S., Lee, R. F., and Benson, A. A.: The presence of unusually high levels of lysophosphatidylethanolamine
1083 in a wax ester-synthesizing copepod (Calanus plumchrus), Biochim. Biophys. Acta BBA-Lipids Lipid Metab.,
1084 270, 479–488, 1972.

1085 Pearson, A. and Ingalls, A. E.: Assessing the use of archaeal lipids as marine environmental proxies, Annu. Rev.
1086 Earth Planet. Sci., 41, 2013.

1087 Periasamy, N., Teichert, H., Weise, K., Vogel, R. F., and Winter, R.: Effects of temperature and pressure on the
1088 lateral organization of model membranes with functionally reconstituted multidrug transporter LmrA, Biochim.
1089 Biophys. Acta BBA-Biomembr., 1788, 390–401, 2009.
1090

1091 Petersen, S. O., Henriksen, K., Blackburn, T. H., and King, G. M.: A comparison of phospholipid and chloroform
1092 fumigation analyses for biomass in soil: potentials and limitations, FEMS Microbiol. Lett., 85, 257–267, 1991.

1093 Pitcher, A. M.: Intact polar lipids of ammonia-oxidizing Archaea: structural diversity application in molecular
1094 ecology, PhD Thesis, Departement Aardwetenschappen, 2011.

1095 Poff, K. E., Leu, A. O., Eppley, J. M., Karl, D. M., and DeLong, E. F.: Microbial dynamics of elevated carbon
1096 flux in the open ocean's abyss, Proc. Natl. Acad. Sci., 118, 2021.

1097 Pond, D. and Harris, R.: The lipid composition of the coccolithophore Emiliania huxleyi and its possible
1098 ecophysiological significance, J. Mar. Biol. Assoc. U. K., 76, 579–594, 1996.

1099 Popendorf, K., Tanaka, T., Pujo-Pay, M., Lagaria, A., Courties, C., Conan, P., Oriol, L., Sofen, L., Moutin, T.,
1100 and Van Mooy, B. A.: Gradients in intact polar diacylglycerolipids across the Mediterranean Sea are related to
1101 phosphate availability, Biogeosciences, 8, 3733–3745, 2011a.

1102 Popendorf, K. J., Lomas, M. W., and Van Mooy, B. A.: Microbial sources of intact polar diacylglycerolipids in
1103 the Western North Atlantic Ocean, Org. Geochem., 42, 803–811, 2011b.

https://doi.org/10.5194/bg-2021-232
Preprint. Discussion started: 3 September 2021

1104 Ratledge, C. and Wilkinson, S. G.: Microbial lipids, Academic press, 1988.

1105 Rex, M. A., Etter, R. J., Morris, J. S., Crouse, J., McClain, C. R., Johnson, N. A., Stuart, C. T., Deming, J. W.,
1106 Thies, R., and Avery, R.: Global bathymetric patterns of standing stock and body size in the deep-sea benthos,
1107 Mar. Ecol. Prog. Ser., 317, 1–8, 2006.

1108 Řezanka, T. and Sigler, K.: Odd-numbered very-long-chain fatty acids from the microbial, animal and plant
1109 kingdoms, Prog. Lipid Res., 48, 206–238, 2009.

1110 Řezanka, T., Viden, I., Go, J., Dor, I., and Dembitsky, V.: Polar lipids and fatty acids of three wild cyanobacterial
1111 strains of the genus Chroococcidiopsis, Folia Microbiol. (Praha), 48, 781–786, 2003.

1112 Rossel, P. E., Elvert, M., Ramette, A., Boetius, A., and Hinrichs, K.-U.: Factors controlling the distribution of
1113 anaerobic methanotrophic communities in marine environments: evidence from intact polar membrane lipids,
1114 Geochim. Cosmochim. Acta, 75, 164–184, 2011.

1115 Rütters, H., Sass, H., Cypionka, H., and Rullkötter, J.: Monoalkylether phospholipids in the sulfate-reducing
1116 bacteria Desulfosarcina variabilis and Desulforhabdus amnigenus, Arch. Microbiol., 176, 435–442, 2001.

1117 Sabbatini, A., Morigi, C., Negri, A., and Gooday, A. J.: Soft-shelled benthic foraminifera from a hadal site (7800
1118 m water depth) in the Atacama Trench (SE Pacific): preliminary observations, J. Micropalaeontology, 21, 131–
1119 135, 2002.

1120 Sakurai, I., Shen, J.-R., Leng, J., Ohashi, S., Kobayashi, M., and Wada, H.: Lipids in oxygen-evolving
1121 photosystem II complexes of cyanobacteria and higher plants, J. Biochem. (Tokyo), 140, 201–209, 2006.

1122 Sato, N.: Betaine lipids, Bot. Mag. Shokubutsu-Gaku-Zasshi, 105, 185–197, 1992.

1123 Sato, N., Hagio, M., Wada, H., and Tsuzuki, M.: Requirement of phosphatidylglycerol for photosynthetic function
1124 in thylakoid membranes, Proc. Natl. Acad. Sci., 97, 10655–10660, 2000.

1125 Schauberger, C., Middelboe, M., Larsen, M., Peoples, L. M., Bartlett, D. H., Kirpekar, F., Rowden, A. A.,
1126 Wenzhöfer, F., Thamdrup, B., and Glud, R. N.: Spatial variability of prokaryotic and viral abundances in the
1127 Kermadec and Atacama Trench regions, Limnol. Oceanogr., 2021.

1128 Schneider, W., Fuenzalida, R., Garcés-Vargas, J., Bravo, L., and Lange, C.: Extensión vertical y horizontal de la
1129 zona de mínima oxígeno en el Pacífico Sur Oriental, Gayana Concepc., 70, 79–82, 2006.

1130 Schouten, S., Middelburg, J. J., Hopmans, E. C., and Damsté, J. S. S.: Fossilization and degradation of intact polar
1131 lipids in deep subsurface sediments: a theoretical approach, Geochim. Cosmochim. Acta, 74, 3806–3814, 2010.

1132 Schubotz, F., Wakeham, S. G., Lipp, J. S., Fredricks, H. F., and Hinrichs, K.-U.: Detection of microbial biomass
1133 by intact polar membrane lipid analysis in the water column and surface sediments of the Black Sea, Environ.
1134 Microbiol., 11, 2720–2734, 2009a.

https://doi.org/10.5194/bg-2021-232
Preprint. Discussion started: 3 September 2021

1135 Schubotz, F., Wakeham, S. G., Lipp, J. S., Fredricks, H. F., and Hinrichs, K.-U.: Detection of microbial biomass
1136 by intact polar membrane lipid analysis in the water column and surface sediments of the Black Sea, Environ.
1137 Microbiol., 11, 2720–2734, 2009b.

1138 Schubotz, F., Meyer-Dombard, D., Bradley, A. S., Fredricks, H. F., Hinrichs, K.-U., Shock, E., and Summons, R.
1139 E.: Spatial and temporal variability of biomarkers and microbial diversity reveal metabolic and community
1140 flexibility in Streamer Biofilm Communities in the Lower Geyser Basin, Yellowstone National Park, Geobiology,
1141 11, 549–569, 2013.

1142 Schubotz, F., Xie, S., Lipp, J. S., Hinrichs, K.-U., and Wakeham, S. G.: Intact polar lipids in the water column of
1143 the eastern tropical North Pacific: abundance and structural variety of non-phosphorus lipids, Biogeosciences, 15,
1144 6481–6501, 2018a.

1145 Schubotz, F., Xie, S., Lipp, J. S., Hinrichs, K.-U., and Wakeham, S. G.: Intact polar lipids in the water column of
1146 the eastern tropical North Pacific: abundance and structural variety of non-phosphorus lipids, Biogeosciences, 15,
1147 6481–6501, 2018b.

1148 Schwestermann, T., Eglinton, T., Haghipour, N., McNichol, A., Ikehara, K., and Strasser, M.: Event-dominated
1149 transport, provenance, and burial of organic carbon in the Japan Trench, Earth Planet. Sci. Lett., 563, 116870,
1150 2021.

1151 Sebastián, M., Smith, A. F., González, J. M., Fredricks, H. F., Van Mooy, B., Koblížek, M., Brandsma, J., Koster,
1152 G., Mestre, M., Mostajir, B., and others: Lipid remodelling is a widespread strategy in marine heterotrophic
1153 bacteria upon phosphorus deficiency, ISME J., 10, 968–978, 2016.

1154 Shaw, N.: Lipid composition as a guide to the classification of bacteria, Adv. Appl. Microbiol., 17, 63–108, 1974.

1155 Siegenthaler, P.-A.: Molecular organization of acyl lipids in photosynthetic membranes of higher plants, in: Lipids
1156 in photosynthesis: structure, function and genetics, Springer, 119–144, 1998.

1157 Siliakus, M. F., van der Oost, J., and Kengen, S. W.: Adaptations of archaeal and bacterial membranes to variations
1158 in temperature, pH and pressure, Extremophiles, 21, 651–670, 2017.

1159 Smith, C.: Chemosynthesis in the deep-sea: life without the sun, Biogeosciences Discuss., 9, 17037–17052, 2012.

1160 Sohlenkamp, C., López-Lara, I. M., and Geiger, O.: Biosynthesis of phosphatidylcholine in bacteria, Prog. Lipid
1161 Res., 42, 115–162, 2003.

1162 Somero, G. N.: Adaptations to high hydrostatic pressure., Annu. Rev. Physiol., 54, 557–577, 1992.

1163 Stockton, W. L. and DeLaca, T. E.: Food falls in the deep sea: occurrence, quality, and significance, Deep Sea
1164 Res. Part Oceanogr. Res. Pap., 29, 157–169, 1982.

1165 Sturt, H. F., Summons, R. E., Smith, K., Elvert, M., and Hinrichs, K.-U.: Intact polar membrane lipids in
1166 prokaryotes and sediments deciphered by high-performance liquid chromatography/electrospray ionization

https://doi.org/10.5194/bg-2021-232
Preprint. Discussion started: 3 September 2021

multistage mass spectrometry—new biomarkers for biogeochemistry and microbial ecology, Rapid Commun. Mass Spectrom., 18, 617–628, 2004.

Suzuki, R. and Shimodaira, H.: Pvclust: an R package for assessing the uncertainty in hierarchical clustering, Bioinformatics, 22, 1540–1542, 2006.

Ta, K., Peng, X., Xu, H., Du, M., Chen, S., Li, J., and Zhang, C.: Distributions and sources of glycerol dialkyl glycerol tetraethers in sediment cores from the Mariana subduction zone, J. Geophys. Res. Biogeosciences, 124, 857–869, 2019.

Tamburini, C., Boutrif, M., Garel, M., Colwell, R. R., and Deming, J. W.: Prokaryotic responses to hydrostatic pressure in the ocean–a review, Environ. Microbiol., 15, 1262–1274, 2013.

Tarn, J., Peoples, L. M., Hardy, K., Cameron, J., and Bartlett, D. H.: Identification of free-living and particle-associated microbial communities present in hadal regions of the Mariana Trench, Front. Microbiol., 7, 665, 2016.

Thompson Jr, G. A.: Lipids and membrane function in green algae, Biochim. Biophys. Acta BBA-Lipids Lipid Metab., 1302, 17–45, 1996.

Turnewitsch, R., Falahat, S., Stehlikova, J., Oguri, K., Glud, R. N., Middelboe, M., Kitazato, H., Wenzhöfer, F., Ando, K., Fujio, S., and others: Recent sediment dynamics in hadal trenches: evidence for the influence of higher-frequency (tidal, near-inertial) fluid dynamics, Deep Sea Res. Part Oceanogr. Res. Pap., 90, 125–138, 2014.

Van Mooy, B. A. and Fredricks, H. F.: Bacterial and eukaryotic intact polar lipids in the eastern subtropical South Pacific: water-column distribution, planktonic sources, and fatty acid composition, Geochim. Cosmochim. Acta, 74, 6499–6516, 2010.

Van Mooy, B. A., Rocap, G., Fredricks, H. F., Evans, C. T., and Devol, A. H.: Sulfolipids dramatically decrease phosphorus demand by picocyanobacteria in oligotrophic marine environments, Proc. Natl. Acad. Sci., 103, 8607–8612, 2006.

Van Mooy, B. A., Fredricks, H. F., Pedler, B. E., Dyhrman, S. T., Karl, D. M., Koblížek, M., Lomas, M. W., Mincer, T. J., Moore, L. R., Moutin, T., and others: Phytoplankton in the ocean use non-phosphorus lipids in response to phosphorus scarcity, Nature, 458, 69–72, 2009.

Vardi, A., Van Mooy, B. A., Fredricks, H. F., Popendorf, K. J., Ossolinski, J. E., Haramaty, L., and Bidle, K. D.: Viral glycosphingolipids induce lytic infection and cell death in marine phytoplankton, Science, 326, 861–865, 2009.

Vargas, C. A., Cantarero, S. I., Sepúlveda, J., Galán, A., De Pol-Holz, R., Walker, B., Schneider, W., Farías, L., D'Ottone, M. C., Walker, J., and others: A source of isotopically light organic carbon in a low-pH anoxic marine zone, Nat. Commun., 12, 1–11, 2021.

Volkman, J., Jeffrey, S., Nichols, P., Rogers, G., and Garland, C.: Fatty acid and lipid composition of 10 species of microalgae used in mariculture, J. Exp. Mar. Biol. Ecol., 128, 219–240, 1989.

https://doi.org/10.5194/bg-2021-232
Preprint. Discussion started: 3 September 2021

1200 Wada, H. and Murata, N.: Membrane lipids in cyanobacteria, in: Lipids in photosynthesis: structure, function and
1201 genetics, Springer, 65–81, 1998.

1202 Wada, H. and Murata, N.: The essential role of phosphatidylglycerol in photosynthesis, Photosynth. Res., 92,
1203 205–215, 2007.

1204 Wakeham, S. G., Lee, C., Farrington, J. W., and Gagosian, R. B.: Biogeochemistry of particulate organic matter
1205 in the oceans: results from sediment trap experiments, Deep Sea Res. Part Oceanogr. Res. Pap., 31, 509–528,
1206 1984.

1207 Wakeham, S. G., Amann, R., Freeman, K. H., Hopmans, E. C., Jørgensen, B. B., Putnam, I. F., Schouten, S.,
1208 Damsté, J. S. S., Talbot, H. M., and Woebken, D.: Microbial ecology of the stratified water column of the Black
1209 Sea as revealed by a comprehensive biomarker study, Org. Geochem., 38, 2070–2097, 2007.

1210 Wakeham, S. G., Turich, C., Schubotz, F., Podlaska, A., Li, X. N., Varela, R., Astor, Y., Saenz, J. P., Rush, D.,
1211 Damste, J. S. S., and others: Biomarkers, chemistry and microbiology show chemoautotrophy in a multilayer
1212 chemocline in the Cariaco Basin, Deep Sea Res. Part Oceanogr. Res. Pap., 63, 133–156, 2012.

1213 Warnes, G., Bolker, B., Bonebakker, L., Gentleman, R., Liaw, W., Lumley, T., and others: gplots: various R
1214 programming tools for plotting data. R package version 2.16. 0. 2015, 2015.

1215 Warton, D. I., Wright, S. T., and Wang, Y.: Distance-based multivariate analyses confound location and dispersion
1216 effects, Methods Ecol. Evol., 3, 89–101, 2012.

1217 Weijers, J. W., Schouten, S., van den Donker, J. C., Hopmans, E. C., and Damsté, J. S. S.: Environmental controls
1218 on bacterial tetraether membrane lipid distribution in soils, Geochim. Cosmochim. Acta, 71, 703–713, 2007.

1219 Wenzhöfer, F., Oguri, K., Middelboe, M., Turnewitsch, R., Toyofuku, T., Kitazato, H., and Glud, R. N.: Benthic
1220 carbon mineralization in hadal trenches: Assessment by in situ O2 microprofile measurements, Deep Sea Res.
1221 Part Oceanogr. Res. Pap., 116, 276–286, 2016.

1222 Wenzhöfer, F. The Expedition SO261 of the Research Vessel SONNE to the Atacama Trench in the Pacific Ocean
1223 in 2018. Rep Polar Mar Res 729:1–111. 2019

1224 White, D., Bobbie, R., King, J., Nickels, J., and Amoe, P.: Lipid analysis of sediments for microbial biomass and
1225 community structure, in: Methodology for biomass determinations and microbial activities in sediments, ASTM
1226 International, 1979.

1227 Winter, R.: Effect of lipid chain length, temperature, pressure and composition on the lateral organisation and
1228 phase behavior of lipid bilayer/gramicidin mixtures, in: Biophysical Journal, 153A-153A, 2002.

1229 Winter, R. and Jeworrek, C.: Effect of pressure on membranes, Soft Matter, 5, 3157–3173, 2009.

1230 Wörmer, L., Lipp, J. S., Schröder, J. M., and Hinrichs, K.-U.: Application of two new LC–ESI–MS methods for
1231 improved detection of intact polar lipids (IPLs) in environmental samples, Org. Geochem., 59, 10–21, 2013.

https://doi.org/10.5194/bg-2021-232
Preprint. Discussion started: 3 September 2021

1232 Xu, Y., Ge, H., and Fang, J.: Biogeochemistry of hadal trenches: Recent developments and future perspectives,
1233 Deep Sea Res. Part II Top. Stud. Oceanogr., 155, 19–26, 2018.

1234 Xu, Y., Jia, Z., Xiao, W., Fang, J., Wang, Y., Luo, M., Wenzhöfer, F., Rowden, A. A., and Glud, R. N.: Glycerol
1235 dialkyl glycerol tetraethers in surface sediments from three Pacific trenches: Distribution, source and
1236 environmental implications, Org. Geochem., 147, 104079, 2020.

1237 Xu, Y., Li, X., Luo, M., Xiao, W., Fang, J., Rashid, H., Peng, Y., Li, W., Wenzhöfer, F., Rowden, A. A., and
1238 others: Distribution, Source, and Burial of Sedimentary Organic Carbon in Kermadec and Atacama Trenches, J.
1239 Geophys. Res. Biogeosciences, 126, e2020JG006189, 2021.

1240 Yano, Y., Nakayama, A., Ishihara, K., and Saito, H.: Adaptive changes in membrane lipids of barophilic bacteria
1241 in response to changes in growth pressure, Appl. Environ. Microbiol., 64, 479–485, 1998.

1242 Zhong, H., Lehtovirta-Morley, L., Liu, J., Zheng, Y., Lin, H., Song, D., Todd, J. D., Tian, J., and Zhang, X.-H.:
1243 Novel insights into the Thaumarchaeota in the deepest oceans: their metabolism and potential adaptation
1244 mechanisms, Microbiome, 8, 1–16, 2020.

1245 Zhukova, N. V.: Variation in microbial biomass and community structure in sediments of Peter the Great Bay
1246 (Sea of Japan/East Sea), as estimated from fatty acid biomarkers, Ocean Sci. J., 40, 34–42, 2005.